"SIMION STOILOW"
INSTITUTE OF MATHEMATICS
OF THE ROMANIAN ACADEMY

CONTRIBUTIONS TO THE STUDY OF ORBITAL ERRORS OF THE GPS SATELLITES DUE TO NON-GRAVITATIONAL PERTURBATIONS

Ph.D THESIS

Summary

Sergiu LUPU

SUPERVISOR:
C.S. I dr. Gabriela MARINOSCHI

BUCHAREST
2014

CONTENTS

1. INTRODUCTION

Since the beginning of time, man has looked up to the sky, which has been an inexhaustible source of questions, myths and legends. Personification of nature and natural phenomena, was the first shy attempt of the primitive man to explain the apparently meaningless world they saw.

Until 500 years ago, people thought the earth was the center of the universe, for a pretty obvious reason: the Moon was orbiting the Earth, and there is no evidence that the Sun was not doing the same. The planets could be seen revolving around the Earth, although at times they seemed to be going the way back for several weeks if not months.

Since the nineteenth century to the present a lot of astronomers and mathematicians have contributed to the evolution and development of astronomy.

The early sailors used to keep the land in view. Sailors that knew the region well were used, relying on many previous passes through the same place: the recognition of rocks, stones surveys tied up to ropes to avoid shallow waters near the land, following the direction of movement of clouds, sea currents recognition, using winds both for sailing and for the recognition of the region where they operate. When the shore was not in view, orientation was made after Sun at daytime and after the stars at night time.

Tales of Miletus says that the Ionian sailors were trained to recognize the constellation Ursa Minor 600 years BC.

Christopher Columbus crossed the Atlantic using astronomical observations, being thus worshiped by the natives of Santa Gloria, in Jamaica Bay after he had predicted the lunar eclipse of February 29, 1504.

In celestial navigation, the navigation landmarks are the celestial bodies (the Sun, the Moon, the planets and the stars); they are easily observed and identified as they form a natural infrastructure.

Celestial navigation markers are localized for a certain observation hour using their ephemeris (paper or electronic). The measurements for celestial bodies are made using a sextant or a theodolite.

Launching of the first artificial satellite (Sputnik) on October 4 1957 by Russia (USSR at that time) had a great scientific importance, being the road opener for many space missions up to the present date.

In 1973, the U.S. Department of Defense wanted to create a spatial positioning system, known as NAVSTAR / GPS (NAVigation System with Timing And Ranging / Global Positioning System).

The first targets aiming at the system were military targets. Further on, the US Congress required promotion of "civil" facilities of the system. This process was pushed forward by the marketing of the first GPS receiver, called "Macrometer" used for geodetic measurements.

For determining the terrestrial position the satellite navigation uses the same principle as celestial navigation. In order to determine the ship's precise position with the help of the satellite navigation system, measurements of four pseudo-distances at four different satellites are required.

For a better precision in the observatory's position it is necessary to know, as accurately as possible, the position of the artificial satellite. Upon a satellite act a series of perturbations that, depending on their nature, are classified as gravitational and non-gravitational perturbations

Accurate modeling of equations of such perturbations ultimately leads to a more precise determination of the observatory's position.

This research paper, which is part of the research topics within the Astronomical Institute of the Romanian Academy, aims to address and investigate the following issues related to the movement GPS satellites:

- developing models of perturbation accelerations that influence the motion of GPS satellites, determining the order of magnitude, and establishing a criterion for their inclusion in the dynamic model;
- study of the analytical method for calculating the influence of gravitational and non gravitational acceleration perturbations in the oscillatory elements of the GPS satellites;
- study, through numerical applications, of the errors of GPS satellites orbit, induced by gravitational and non-gravitational perturbation accelerations, with emphasis on non-gravitational accelerations;
- qualitative study of GPS satellites movement.

The paper is divided into six chapters as follows:

Chapter I present NAVSTAR/GPS, GPS satellite system, the identification of GPS technology applications, reference systems and time scales required by the study of disruptive forces acting on GPS satellites.

Chapter II presents a quantitative analysis of GPS satellites motion under the influence of gravitational and non-gravitational perturbations.

Chapter III contains the quantitative analysis of non gravitational perturbations: direct solar radiation pressure, indirect solar radiation pressure, anisotropic thermal emission, antenna emission, and empirical models of solar radiation pressure.

Chapter IV presents the author's original method using Runge–Kutta integration algorithm of order 4, for determining gravitational perturbation accelerations that act upon GPS satellites and the effects produced by the non-gravitational perturbations to the orbital elements of the satellites.

Chapter V is a qualitative or geometric study of GPS satellites motion. This is a new approach which applies the geometric method to analyze dynamic systems whose initiator is Poincare, for the study of GPS satellites motion. The analysis is not limited to GPS satellites alone; it also takes into account a multitude of cases, resulting in a comprehensive analysis of satellite motion.

Chapter VI contains a brief overview of important data and conclusions presented in previous chapters, highlighting the main results obtained by the author.

2. QUANTITATIVE ANALYSIS OF NAVSTAR/GPS SATELLITE MOTION

2.1. Equations of GPS satellite motions

Vector differential equation of relative motion of a satellite around the central body, in the absence of any disturbing influences, has the form (Brouwer and Clemence 1961, Pal and Ureche 1983):

$$\frac{d^2\vec{r}}{dt^2} = -\mu \frac{\vec{r}}{r^3} \tag{2.1}$$

and the scalar equations are:

$$\frac{d^2x}{dt^2} = -\mu \frac{x}{r^3}, \qquad \frac{d^2y}{dt^2} = -\mu \frac{y}{r^3}, \qquad \frac{d^2z}{dt^2} = -\mu \frac{z}{r^3} \tag{2.2}$$

The analytical integration process of the of 3 differential equations system, of order 2 reveals 4 prime integrals (the energy integral and the surface integrals), the orbit equation, and equations of motion of the satellite on the orbital plane, as well as 6 integration constants determinable form conditions (initial positions and initial velocity):

a - the semi-major axis
e - the eccentricity
i - the inclination
ω - the mean anomaly
Ω - the perigee argument
M - the longitude of the ascending node

Those six constants of integration are actually kepleriene elliptical orbit parameters and define the position of the orbit in inertial space (i, Ω), the orientation of the orbit in its plane (ω), the shape of the orbit (a, e), and orbital position (M). The only parameter that depends on the orbital time is average anomaly. As a result, the place can be used when moving the perigee (t_0).

2.2 Functions of the disturbing force

As known, a significant number of disturbing forces (accelerations) act upon an artificial satellite of the Earth; they are of a much smaller magnitude than the central force (acceleration), and in time they significantly influence the dynamics of the satellite.

For first-order linear theory development it is necessary to express the main categories of disturbing force functions in terms orbital elements, while for the numerical integration of the differential equation (2.2) of the disturbed motion, it is necessary that they be expressed in terms of cartesian coordinates.

Depending on their nature there can be **gravitational** disturbing accelerations and **non-gravitational** disturbing accelerations.

Gravitational disturbing accelerations:

- the Earth's gravitational field is not centered;
- the Sun’s and the Moon’s gravitational pull;
- the indirect effect of the attraction of the Sun and the Moon (the indirect tidal effect);
- the gravitational pull of other planets;
- relativistic effects;

Non-gravitational acceleration disturbance:

- direct solar radiation pressure;
- pressure of solar radiation re-emitted by the Earth's surface (the Earth’s albedo);
- the Poynting–Robertson effect;
- aerodynamic stopping;
- solar wind;
- other accelerations, such as inter-planetary dust, heat radiation of the satellite, etc..

The magnitude of disturbing accelerations depends, on one hand on the nature of the phenomenon that generates term, and on the other hand on the values of orbital satellite parameters.

Any modification of a parameter of the satellite orbit can be written as (Escobal, 1965):

$$u(t) = u(t_0) + \frac{du}{dt}(t - t_0) + k_1 \cdot \cos(2\omega) + k_2 \cdot \sin(2v + \omega) + k_3 \cdot \cos(2v) \qquad (2.3)$$

where:

v - true anomaly;

k1, k2, k3 - sums and products depending on the major semi-axis, eccentricity, and inclination.

The effect of a disturbing acceleration can be:

- **secular**, $\frac{du}{dt}(t - t_0)$ i.e. it has linear evolution and it is cumulative over time;
- **long – periodic,** $k_1 \cdot \cos(2\omega)$ where the disturbance amplitude increases and decreases with a certain defined interval of time, this being higher than the orbital period;
- **short - periodic**, $k_3 \cdot \cos(2v)$ if the period of variation is shorter than the orbital perio
- **mixed - periodical**, $k_2 \cdot \sin(2v + \omega)$ combination of disturbances with long and short periods (intervals).

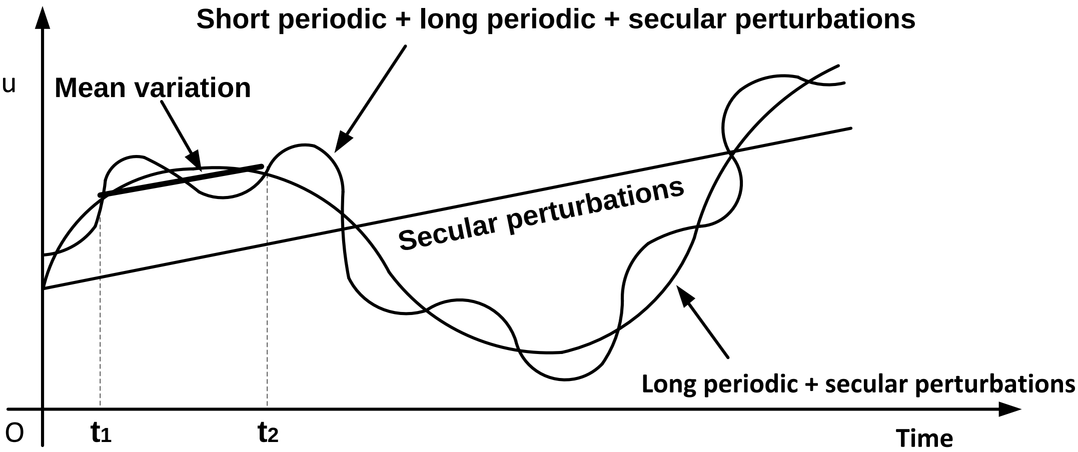

Figure 2.1 Perturations type

3. NUMERICAL RESULTS OF QUANTITATIVE ANALYSIS OF NAVSTAR/GPS SATELLITE ORBIT

3.1 Calculation of the GPS satellite orbit

For calculating the orbit GPS satellites, two methods are used. The first method called the analytical method is based on analytical solutions of Lagrange's planetary equations, expressed in terms of Keplerian orbital elements. The second method is based on the numerical solution of differential equation 2nd order perturbed relative motion in Cartesian coordinates, called numerical method.

The analytical solution used to calculate the precise GPS orbit short arcs is an extension of the 1st order perturbation theory. In order to determine the effects introduced by the 2^{nd} zonal harmonic (C20 or J_2 coefficient) 2^{nd} order perturbations must be included; as a principle, this requires the second solution of Lagrange planetary equations, using the solution 1st order (linear) to evaluate the right member of this equation.

The numerical solution of GPS satellites orbit is based on direct numerical integration of order 2 differential equations of perturbed relative motion, in Cartesian coordinates.

This method can be found in two forms: Cowell method and Encke method. The advantage of numerical method is the simple formulation of movement equations.

In Cartesian coordinates, they have the following form:

$$\ddot{x}_i = -\frac{\mu}{r^2} \cdot \frac{x_i}{r} + \frac{\partial \Re}{\partial x_i} \quad \text{for } i = 1, 2, 3 \tag{3.1}$$

in which *r i*s the geocentric vector radius, and $\frac{\partial \Re}{\partial x_i}$ is the sum of the disturbing accelerations caused by the fact that the terrestrial gravitational field is not centered, any by the fact that the Moon – Sun gravitational interference, as well as by the solar radiation pressure.

The coordinates x_i are defined in an inertial, geocentric equatorial reference system. Equations of motion are complete when each disturbing acceleration is measured and converted into the reference system.

3.2 The Runge-Kutta method

In general, with defined initial conditions (namely position $\vec{x}_0$ and velocity $\dot{\vec{x}}_0$ at t_0 launch time) equations (4.16) can be integrated numerically. The Keplerian orbit is taken as reference. Thus, only the small differences between total acceleration and central acceleration must be integrated. Integration will result into an increase (incremental) $d\vec{x}$ which provides the correct position when it is summed up with the position vector calculated on the reference ellipse. The differential equations of order 2 usually result into a 2 differential equation system, of order 1, as follows:

$$\underline{\dot{x}}(t) = \underline{\dot{x}}(t_0) + \int_{t_0}^{t} \left[d\underline{\ddot{x}}(t_0) - \frac{\mu}{r^3(t_0)} \underline{x}(t_0) \right] dt \tag{3.1}$$

$$\underline{x}(t) = \underline{x}(t_0) + \int_{t_0}^{t} \underline{\dot{x}}(t_0) dt$$

The numerical integration of this system is achieved by applying a Runge-Kutta algorithm of order 4. The principle of the method is the following:

Be $y(x)$ a function defined on the interval $x_1 \le x \le x_2$ and $y' = dy/dx$ the derivative of order 1 with respect to variable x. The general solution of a first order differential equations of the form

$$y' = dy/dx = y'(y, x)$$

results by integration, when assigning an initial numerical value to the integration constant $y_1 = y(x_1)$. Integration interval is divided into *n* equal subdivisions, small enought $\left[\Delta x = (x_2 - x_1)/n\right]$, where *n* is an arbitrary integer. Then, the difference between successive functional values is obtained from the arithmetic mean:

$$\Delta y = y(x + \Delta x) = y(x) = \frac{1}{6}\left[\Delta y^{(1)} + 2\left(\Delta y^{(2)} + \Delta y^{(3)} \right) + \Delta y^{(4)} \right] \tag{3.2}$$

where:

$$\Delta y^{(1)} = y'(y, x)\Delta x$$

$$\Delta y^{(2)} = y'\left(y + \frac{\Delta y^{(1)}}{2}, x + \frac{\Delta x}{2} \right)\Delta x$$

$$\Delta y^{(3)} = y'\left(y + \frac{\Delta y^{(2)}}{2}, x + \frac{\Delta x}{2} \right)\Delta x$$

$$\Delta y^{(4)} = y'(y + \Delta y^{(3)}, x + \Delta x)\Delta x$$

Thus, starting from the initial value y_1 corresponding to argument x_1, the function can be calculated for the successive arguments $x_1 + \Delta x$, $x_2 + \Delta x$, etc.. In the above example, variable x must be interpreted as a variable time (*t*).

This method can be applied to the integration of Newton-Euler, and Lagrange equations system, which are equations of first order. Be Newton-Euler equations as follows:

$$\dot{q}_i = \dot{q}_i\left[q_j, t \right] \equiv \dot{q}_i \left\{ a, e, i, \omega, \Omega, M \right\} \tag{3.3}$$

where q_i is any of the keplerian elements of the satellite. The integration of systerm (2.7) is made in a constant interval of time Δt (small enough), as follows:

$$\begin{aligned}
w_i &= \dot{q}_i\left[q_j(t), t \right] \cdot \Delta t \\
x_i &= \dot{q}_i\left[q_j(t) + \frac{w_j}{2}, t + \frac{\Delta t}{2} \right] \cdot \Delta t \\
y_i &= \dot{q}_i\left[q_j(t) + \frac{x_j}{2}, t + \frac{\Delta t}{2} \right] \cdot \Delta t \\
z_i &= \dot{q}_i\left[q_j(t) + \frac{y_j}{2}, t + \frac{\Delta t}{2} \right] \cdot \Delta t \\
q_i(t + \Delta t) &= q_i(t) + \frac{w_i}{6} + \frac{x_i}{3} + \frac{y_i}{3} + \frac{z_i}{6}
\end{aligned} \tag{3.4}$$

3.3 The Numerical Results of the GPS Satellites Analysis

An unperturbed Keplerian orbit was considered for the initial conditions, on 10th February 2011, UTC 00.00.

xai = 2425.8676; vxai = 3.8327;
yai = -15215.1157; vyai = 0.4529;
zai = 21743.2188; vzai = -0.1055;

θ = 1.0027379093·UT1 + υ_o + $\Delta\Psi$ cosε

UT1 = UTC - dUT1, (dUT1 = 0.162626)

$\upsilon_o = 24110^s{}_{.54841} + 8640184^s{}_{.812866}\cdot T + 0^s{}_{.093104}\cdot T^2 - 6^s{}_{.2}\cdot 10^{-6}\cdot T^3 = 580910482.2$

$$T = \frac{JD}{36525} = \frac{2455602{,}5}{36525} = 67{,}23073237$$

$\Delta\Psi$ cosε = -62.61453881

θ = 1.0027379093*(UT-0.162626) + 580910482.2 - 62.61453881

The values of the arguments for accuracy according to IERS Bulletin:

xp = 0.03428
yp = 0.20863

The order 4 Runge – Kutta algorithm was applied for the integration of undisturbed motion equation (1.1). The software determined, for the selected interval, the values of the vector radius and velocity (r,v), for each integration step, which was then wrote in a text file. The software also solved the problem of Laplace and determined, based on the (r,v) values of the 6 Keplerian elements $(a,\ e,\ i,\ \omega,\ \Omega,\ M)$ and components of accelerations.

The motion of the satellite under observation was considered successively disrupted by a single disturbance: the zonal harmonic J_2, J_3, J_4, J_5, J_6, the gravitational perturbation of the Sun and of the Moon, relativistic effects, and direct solar radiation pressure.

Likewise, the calculation software had as output data the text files corresponding to the orbital elements (r,v) and $(a,\ e,\ i,\ \omega,\ \Omega,\ M)$. For each orbital element the difference was made between the values obtained in the unperturbed case, and the values obtained in case of disturbance, there resulting in orbital element variation under the influence of the disturbance considered. Each variation alone was analyzed separately, and a variation graph was drawn for it.

The orbit integration was performed for a period of 2.1 days (50 hours) and 20.8 days (500 hours) for some disturbances. First the disturbing accelerations acting on a satellite in average orbit (GPS satellite) are exemplified.

Orbital errors induced by main perturbations on the geostationary satellite are then presented.

For determining orbital errors of GPS satellites J_2, J_3, J_4, J_6 și J_{22}, zonal harmonics, Moon, Sun perturbations and solar radiations pressure must be taken into consideration.

Next the effects of the perturbations upon the GPS satellite orbit are analised and synthetised in the following table.

Table 1.1 Numerical values of the perturbative accelerations

Parameter	**GPS satellite**	**Calculation formula** [Km/s^2]
Semi-major axis	26 500 km	
Inclination	55^0	
Central acceleration	5,6 * 10^{-4}	$\frac{\mu}{r^2}$
Perturbation	**Acceleration [Km/s^2]**	**Formula**
J_2 harmonic	2 x 10^{-7}	$3\frac{\mu}{r^2}\frac{a_{ec}^2}{r^2}J_2$
J_3 harmonic	2,3 x 10^{-11}	$4\frac{\mu}{r^2}\frac{a_{ec}^3}{r^3}J_3$
J_4 harmonic	2,5 x 10^{-11}	$5\frac{\mu}{r^2}\frac{a_{ec}^4}{r^4}J_4$
J_5 harmonic	1,1 x 10^{-12}	$6\frac{\mu}{r^2}\frac{a_{ec}^5}{r^5}J_5$
J_6 harmonic	5,6 x 10^{-13}	$7\frac{\mu}{r^2}\frac{a_{ec}^6}{r^6}J_6$
The Sun's gravitational attraction	2,95 x 10^{-8}	$\mu_{3c}\left(\frac{\vec{r}_{3c}-\vec{r}}{(r_{3c}-r)^3}-\frac{\vec{r}_{3c}}{r_{3c}^3}\right)$

The Moon's gravitatioanl attraction	1,95 x 10^{-8}	
Relativistic effects	3,4 x 10^{-12}	$\frac{3\mu^2 a\left(1-e^2\right)}{c^2 r^4}$
Solar radiation pressure	4,4 x 10^{-10}	$k'\frac{A}{m}q\Psi\frac{\vec{r}_{sat}-\vec{r}_{Soare}}{r_{Soare}}$
The Poynting-Robertson efect	6,9 x 10^{-15}	$\frac{r^2}{4c^2m}\sqrt{\frac{GM_sL_s^2}{R^5}}$

3.4 Efects of the Gravitational Perturbations

The Keplerian Orbit

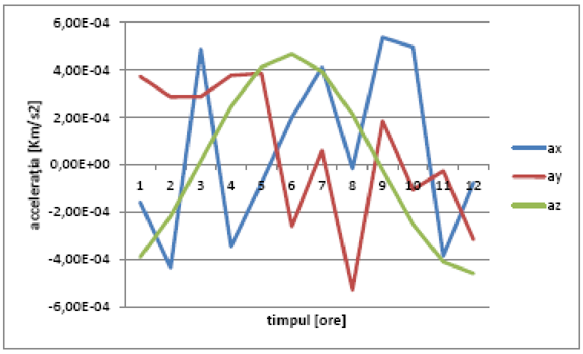

Variaţia componentelor acceleraţiei

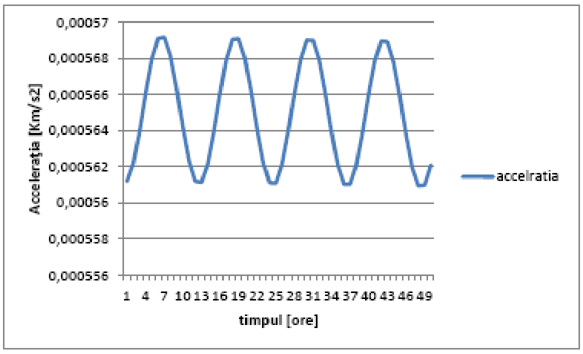

Variaţia acceleraţiei totale

In Keplerian motions without disturbances acceleration has the mean value equal to $5,6\cdot10^{-4}$ Km/s^2.

J_2 Perturbation

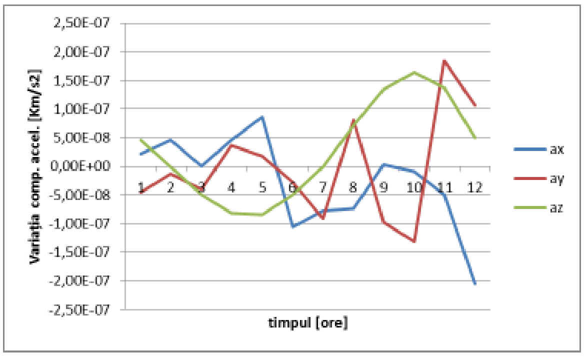

Variaţia componentelor acceleraţiei datorată perturbaţiei J2

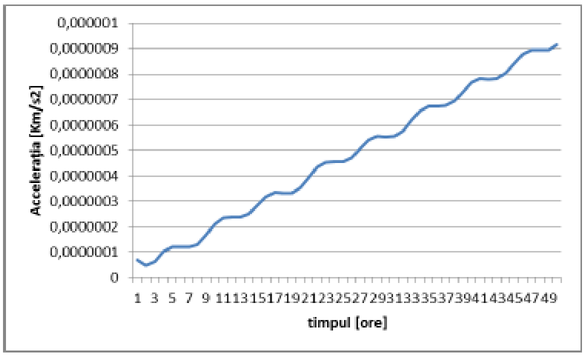

Variaţia acceleraţiei totale datorată perturbaţiei J2

In J_2 perturbation acceleration has a mean value equal to $2\cdot10^{-7}$ Km/s^2.

J_3 Perturbation

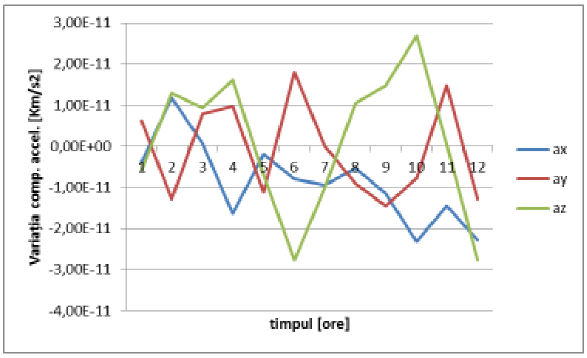

Variația componentelor accelerației datorată perturbației J3

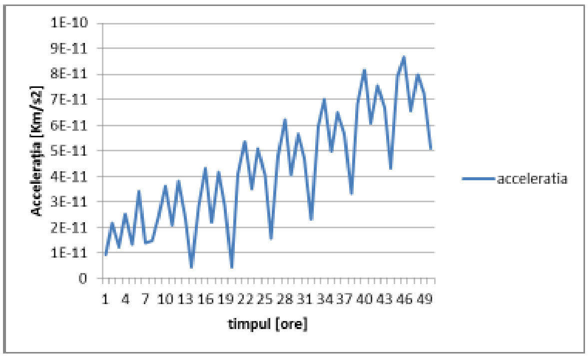

Variația accelerației totale datorată perturbației J3

In J_3 perturbation acceleration has a mean value equal to $2,3 \cdot 10^{-11}$ Km/s^2.

J_4 Perturbation

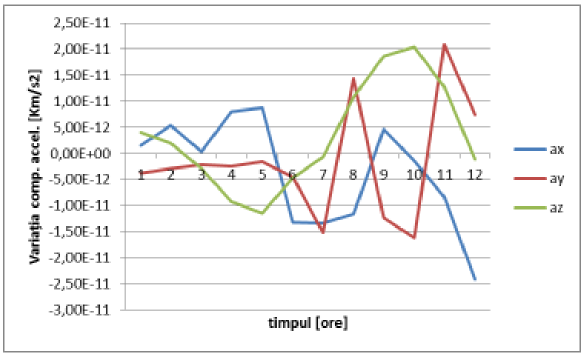

Variația componentelor accelerației datorată perturbației J4

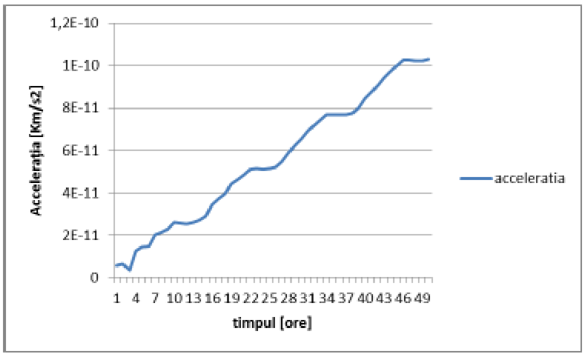

Variația accelerației totale datorată perturbației J4

In J_4 perturbation acceleration has a mean value of $2,5 \cdot 10^{-11}$ Km/s^2.

J_5 Perturbation

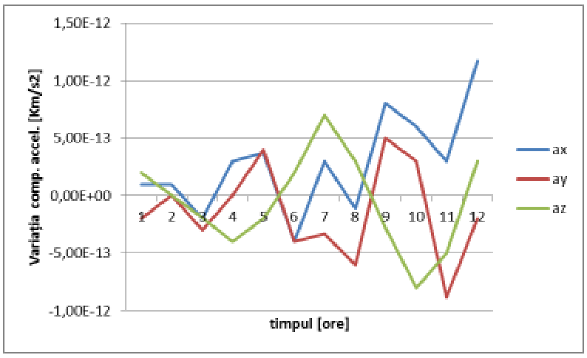

Variația componentelor accelerației datorată perturbației J5

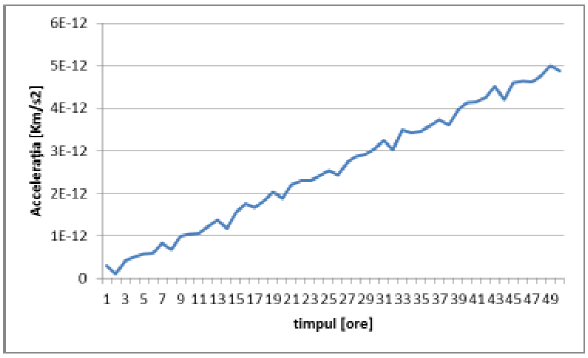

Variația accelerației totale datorată perturbației J5

In J_5 perturbation acceleration has a mean value of $1,1 \cdot 10^{-12}$ Km/s^2.

J_6 Perturbation

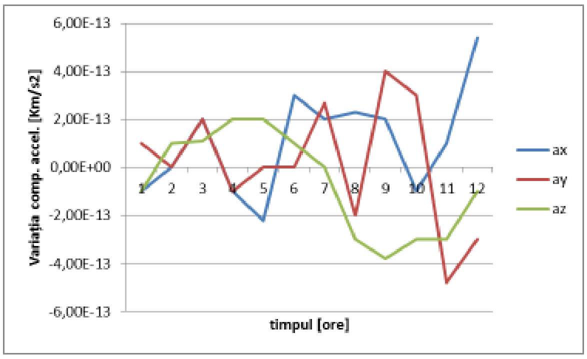

Variația componentelor accelerației datorată perturbației J6

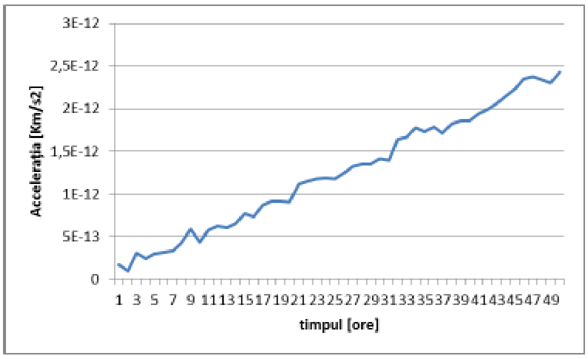

Variația accelerației totale datorată perturbației J6

In J_6 perturbation acceleration has a mean value of $5,6 \cdot 10^{-13}$ Km/s^2.

The Sun's gravitational attraction

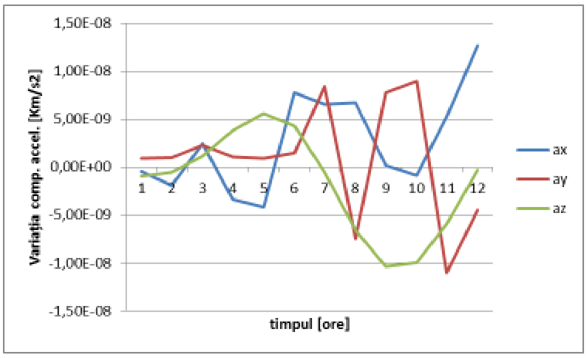

Variația componentelor accelerației datorată atracției gravitaționale a Soarelui

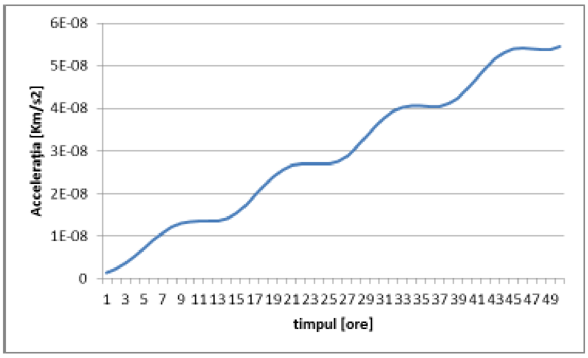

Variația accelerației totale datorată atracției gravitaționale a Soarelui

When the perturbation is produced by the Sun's gravitational attraction the acceleration has a mean value of $2,95 \cdot 10^{-8}$ Km/s^2.

The Moon's gravitatioanl attraction

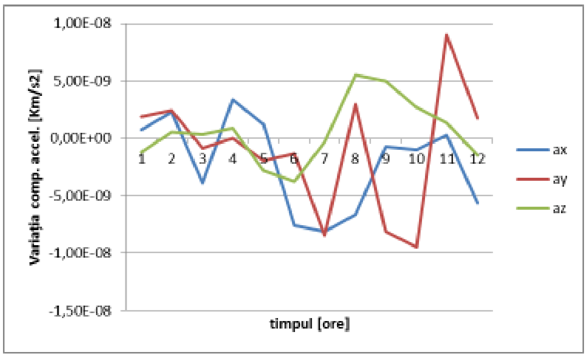

Variația componentelor accelerației datorată atracției gravitaționale a Lunii

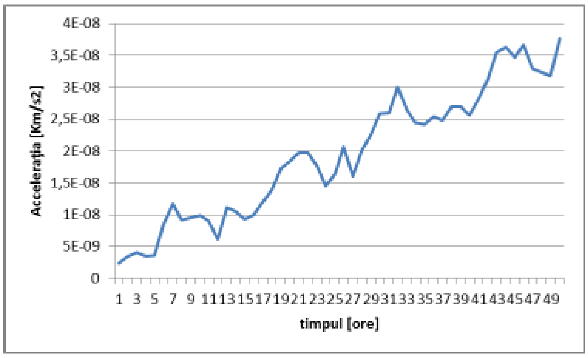

Variația accelerației totale datorată atracției gravitaționale a Lunii

When the perturbation is produced by the Moon's gravitational attraction the acceleration has a mean value of $1,95 \cdot 10^{-8}$ Km/s^2.

Relativistic effects

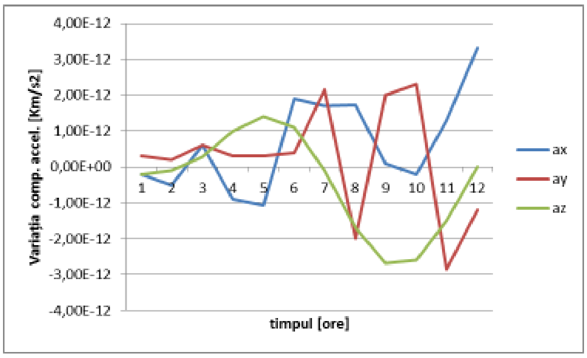

Variaţia componentelor acceleraţiei datorată perturbaţiei efectelor relativiste

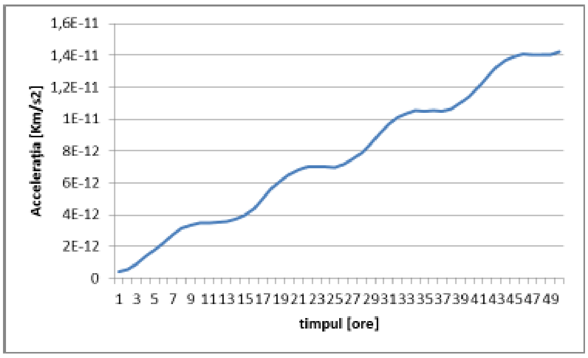

Variaţia acceleraţiei totale datorată perturbaţiei efectelor relativiste

When the perturbation is produced by relativistic effects the acceleration has a mean value of $3,45 \cdot 10^{-12}$ Km/s^2.

3.5 Effects of the non–gravitational perturbations

3.5.1 The direct solar radiation pressure

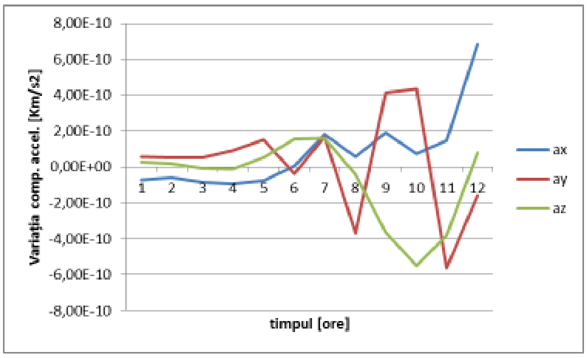

Variaţia componentelor acceleraţiei datorată acţiunii presiunii de radiaţie solară directă

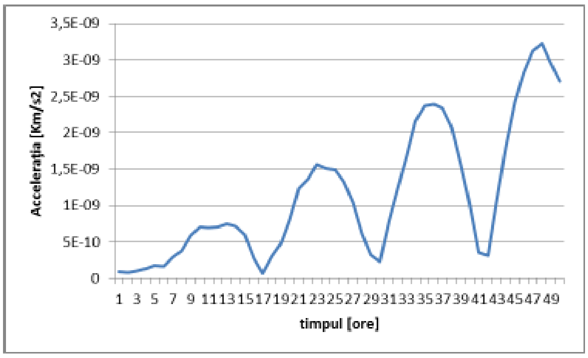

Variaţia acceleraţiei totale datorată acţiunii presiunii de radiaţie solară directă

When the perturbation is produced by the direct radiation pressure the acceleration has a mean value of $4,4 \cdot 10^{-10}$ Km/s^2.

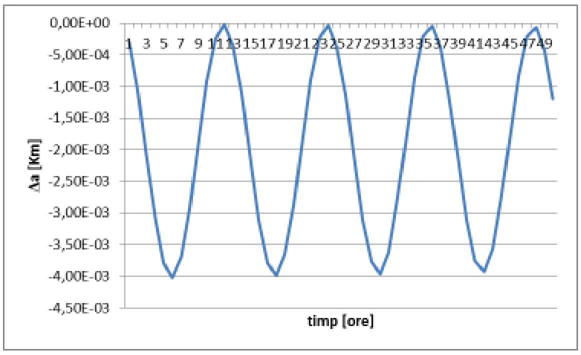

Variația semiaxei mari

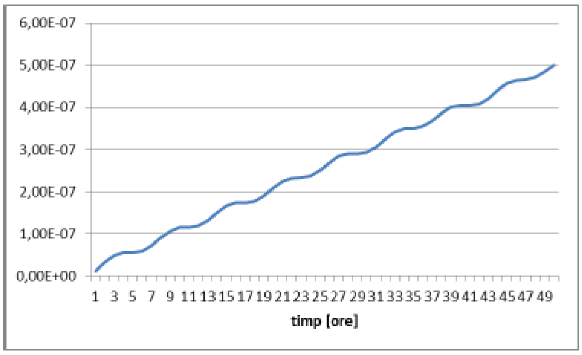

Variația excentricității

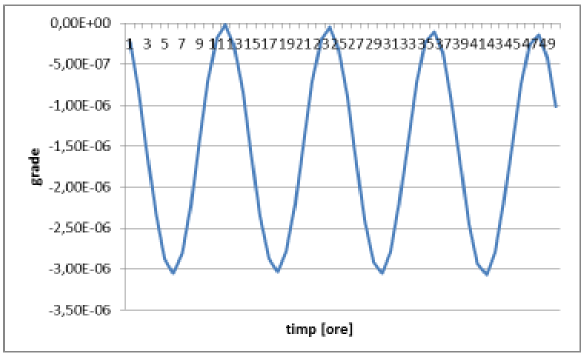

Variația înclinării

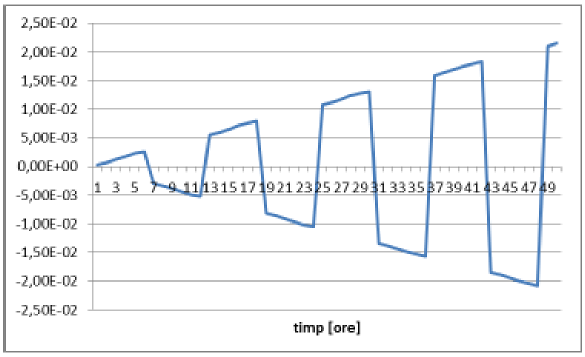

Variația anomaliei medii

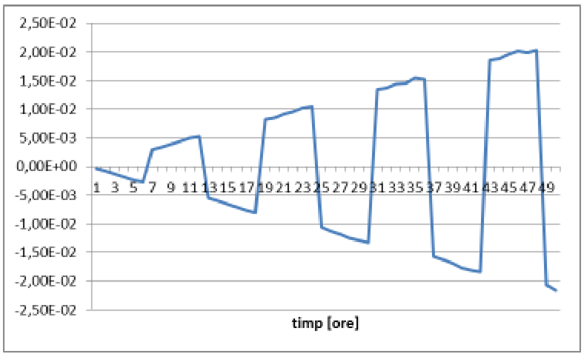

Variația argumentului perigeului

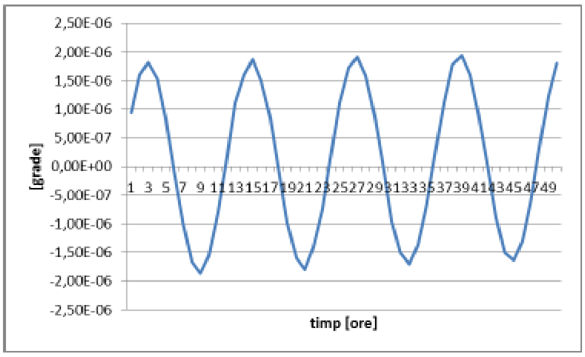

Variația longitudinii nodului ascendent

The semi-major axis has a short-periodic perturbation with a period of 6 hours superimposed on a secular perturbation. For an orbital period, the major semi axis undergoes a variation of 4 meters.

Eccentricity has a secular perturbation superimposed on a short-periodic perturbation with period of 6 hours with the order of magnitude $6 \cdot 10^{-8}$.

The inclination has the same type of disturbance as that of the major semi–major axis, a short-periodic perturbation superimposed on a secular perturbation. The short-period disturbance has a period of 6 hours, and the order of magnitude $3 \cdot 10^{-6}$ degrees. The longitude of the ascending node has short periodic disturbance with a period of 6 hours, and an amplitude of $1,7 \cdot 10^{-6}$ degrees, superimposed on a secular perturbation.

3.5.2 The indirect solar radiation pressure. The Earth's radiation

Reflected Radiation

The Earth's atmosphere reflects some incoming radiation from the Sun, and for making things simple we consider that this radiation is reflected back into space returned by a sphere covered with a Lambertian surface.

The irradiance vector in the direction of the satellite $\vec{r}$, due to the Earth's overall albedo α ,, depends only on the relative position of the satellite, of the Earth and the Sun (angle ψ) and on a satellite located at a height h it has the following form:

$$\vec{E}_{sat}(\psi,h)=\frac{2\alpha}{3\pi^2}\frac{A_E E_{Soare}}{(R_P+h)^2}\left((\pi-\psi)\cos\psi+\sin\psi\right)\vec{r} \qquad (3.5)$$

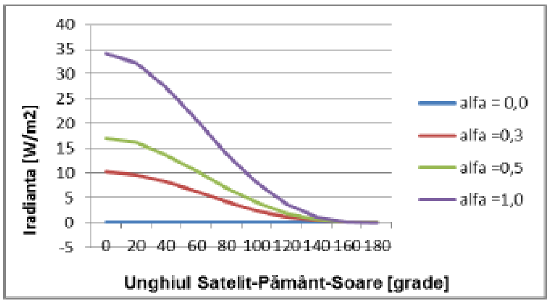

Iradianța datorată radiației reflectată de Pământ

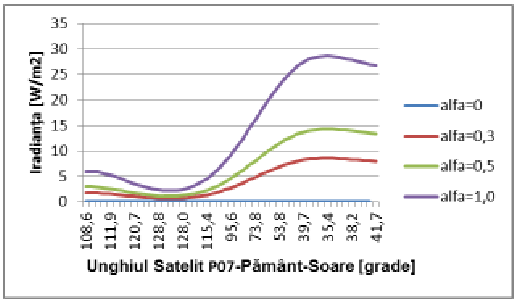

Iradianța datorată radiației reflectată de Pământ pentru satelitul GPS P07

Thus, it is noted that the variation chart of the Earth's irradiance is a sinusoidal curve, and that it decreases once the Earth's albedo is increasing, and the angle ψ between the satellite, the Earth and the Sun increases. For a zero value of the Earth's albedo the irradiance is null (zero).

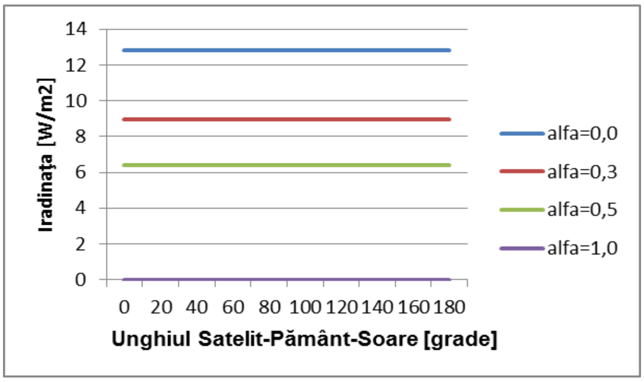

Iradiația datorată radiației emisă de Pământ

Emitted radiation

Incoming radiation from the Sun which intersects the Earth can be determined, and it is $A_E \cdot E_{Soare}$ cu $A_E=\pi R_E^2$. A part of this radiation is immediately reflected in the visible spectrum, one part is absorbed, and another one is re-emitted as infrared radiation (Taylor 2005).

$$E_{sat}(\psi)=\frac{(1-\alpha)}{4\pi}\frac{A_E E_{Soare}}{(R_E+h)^2} \qquad (3.6)$$

the irradiance vector on a satellite located at a height h due to the radiation emitted by the Earth is expressed as:

$$\vec{E}_{sat}(\psi,h) = \frac{(1-\alpha)}{4\pi}\frac{A_E E_{Soare}}{(R_E+h)^2}\vec{r} \qquad (3.7)$$

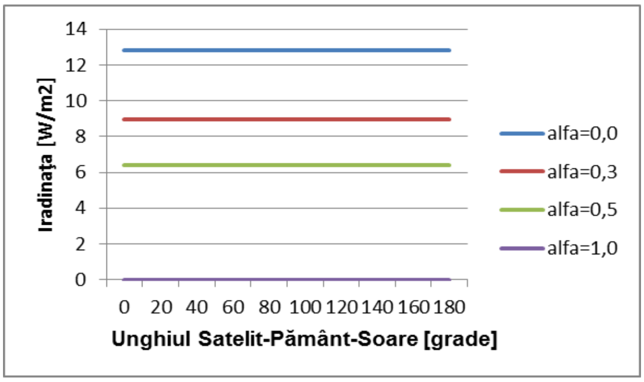

Irradiation due to radiation emitted from the Earth

The graph shows that the irradiance is independent of the angle ψ, is constant taking different values which depend on the value of Earth's albedo. Irradiance has zero value for $\alpha = 1$.

The Earth's Radiation Model

The Earth's radiation model is the sum total of reflected radiation and emitted radiation, and is expressed as:

$$E_{sat}(\psi) = \frac{A_E E_{Soare}}{(R_E+h)^2}\left[\frac{2\alpha}{3\pi^2}\left((\pi-\psi)\cos\psi+\sin\psi\right)+\frac{(1-\alpha)}{4\pi}\right] \qquad (3.8)$$

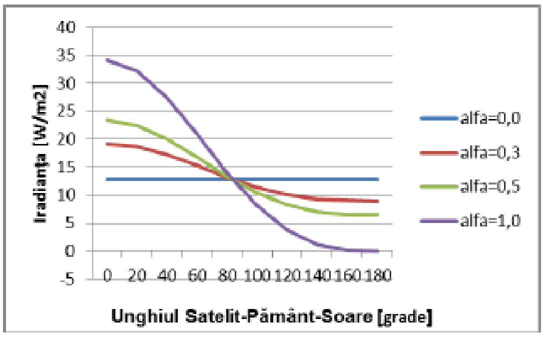

Iradianța totală a Pământului

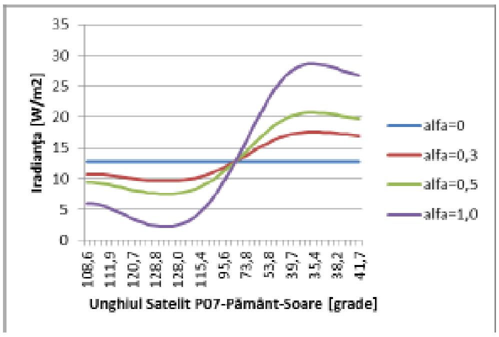

Iradianța totală a Pământului pentru satelitul GPS P07

The albedo model in relation to latitude

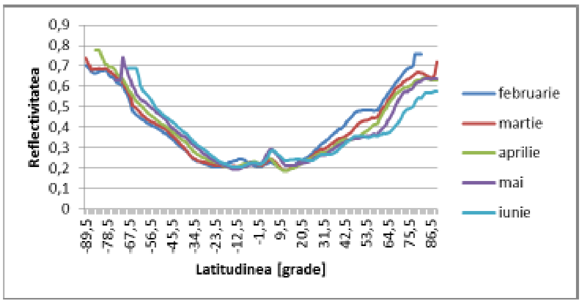

Reflectivitatea februarie – iunie CERES

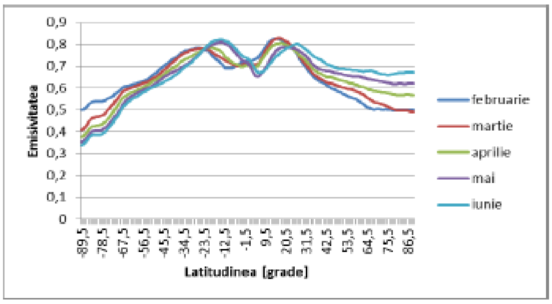

Emisivitatea februarie – iunie CERES

Assuming that reflectivity and emissivity can be written as harmonic developments, in relation to latitude, of the form:

$$\rho(\lambda) = \rho_{const} + \rho_{\cos}\cos\varphi + \rho_{\sin}\sin\varphi \qquad (3.9)$$
$$\varepsilon(\lambda) = \varepsilon_{const} + \varepsilon_{\cos}\cos\varphi + \varepsilon_{\sin}\sin\varphi$$

reflectivity and emissivity coefficients can be determined using the method of least squares.

Tab. 3.1.The estimated coefficients for reflectivity and emissivity for the interval February – June 2011

ρ_{const}	0,737963502
$\rho_{\cos}$	-0,5300641743
$\rho_{\sin}$	-0,026283497
ε_{const}	0,4566176405
$\varepsilon_{\cos}$	0,3057731068
$\varepsilon_{\sin}$	0,0292256524

The acceleration model exerted on GPS satellites

The irradiance vector (*Esat*) or the solar flux (Φ) according to the notation used by Montenbruck and Gill (2000) has the expression:

$$\Phi = \frac{\Delta E}{A\Delta t} \qquad (3.10)$$

it represents the energy transferred through the area A in a time unit. According to Beutler (2005) who says that according to quantum mechanics each frequency photon ν and wavelength $\lambda = c/\nu$ carry energy:

$$E = h\nu \qquad (3.11)$$

and a momentum:

$$p = \frac{E}{c} \qquad (3.12)$$

where h = 6.62 x10-34Js - Planck's constant. Thus, the total momentum for an absorbing body illuminated by the Earth in the time interval Δt is:

$$\Delta p = \frac{\Delta E}{c} = \frac{\Phi}{c} A\Delta t \qquad (3.13)$$

Thus the force acting on a satellite is:

$$F = \frac{\Delta p}{\Delta t} = \frac{\Phi}{c} A \qquad (3.14)$$

and radiation pressure is:

$$P = \frac{\Phi}{c} \qquad (3.15)$$

The GPS satellite on which the radiation pressure of the Earth is acting will be considered as having two forms: it can be either a sphere or a "canonical ball", or in the form of a box with wings (wing box), where the box ("box") is the satellite itself, while the wings are the solar panels. Of particular interest is the transverse section of the satellite, and its optical properties.

The general model of solar radiation pressure emitted by the Earth

The "box-wing" GPS satellite is based on general models of radiation pressure developed by Fliegel (1992) and Hunentobler (2008).

Knowing the area of a flat surface *A*, the mass of the satellite M, the angle θ between the incoming radiation from the earth, and normal to the surface, the Earth's irradiance *E*, the speed of light *c* we can write the three components of acceleration for each area according to Fliegel et al. (1992):

Normal to the surface:

$$\vec{f}_N = \frac{A}{M}\cdot\frac{E}{c}(1+\mu\nu)\cos^2\theta\vec{n} \tag{3.16}$$

Tangent to the surface:

$$\vec{f}_S = \frac{A}{M}\cdot\frac{E}{c}(1+\mu\nu)\sin\theta\cos\theta\vec{t} \tag{3.17}$$

Diffuse:

The radial and non-radial componwent for the solar panels has the following form:

$$f_{\vec{r}} = \frac{A}{M}\cdot\frac{E}{c}|\cos\psi|\left(1+\frac{2}{3}\nu(1-\mu)|\cos\psi|+\mu\nu\cos 2\psi\right) \tag{3.18}$$

$$f_{\vec{r}_\perp} = \frac{A}{M}\cdot\frac{E}{c}\cos\psi\left(\frac{2}{3}\nu(1-\mu)\sin\psi+\mu\nu|\sin 2\psi|\right) \tag{3.19}$$

or, in a more simplified way:

$$f_{\vec{r}} = \frac{E}{Mc}\left[A_{cutie}C_{cutie}+A_{panou}|\cos\psi|\left(1+\frac{2}{3}\nu(1-\mu)|\cos\psi|+\mu\nu\cos 2\psi\right)\right] \tag{3.20}$$

$$f_{\vec{r}_\perp} = \frac{E}{Mc}A_{panou}\cos\psi\left(\frac{2}{3}\nu(1-\mu)\sin\psi+\mu\nu|\sin 2\psi|\right)$$

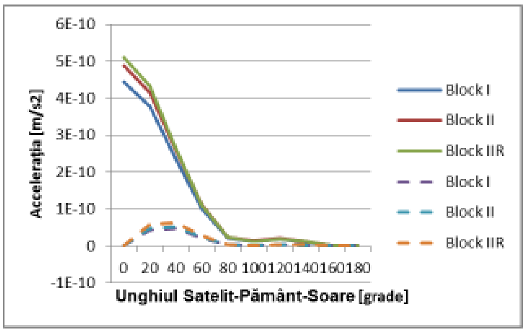

Accelerațiile datorate radiației vizibile reflectate de Pământ, componentele radiale și non-radiale

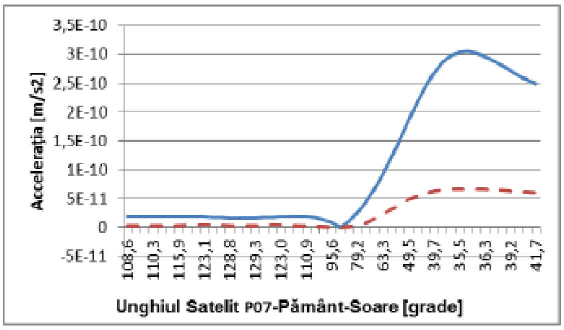

Accelerațiile datorate radiației vizibile reflectate de Pământ, componentele radiale și non-radiale pentru satelitul GPS P07

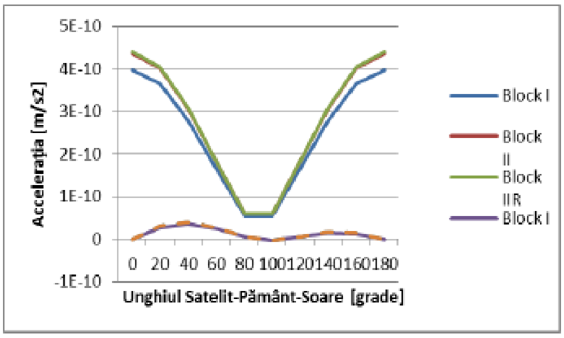

Accelerațiile datorate radiației emise infraroșu de Pământ, componentele radiale și non-radiale

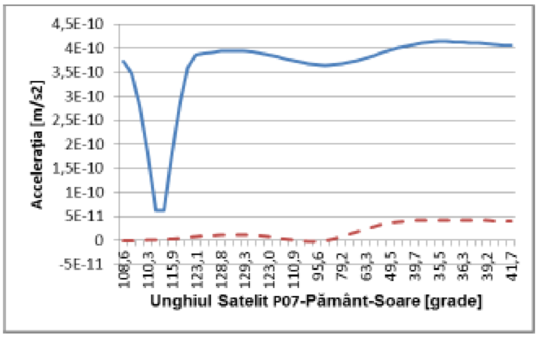

Accelerațiile datorate radiației emise infraroșu de Pământ, componentele radiale și non-radiale asupra satelitului GPS P07

The radial accelerations are represented by a solid line, while the non-radial accelerations are represented by dotted lines.

It can be noted that the radial acceleration achieves its minimum for $\psi = 90°$.

The maximum of teh radial component is achieved for $\psi = 0°$ and $\psi = 180°$.

In the case of non-radial component there still is a maximum and a minimum for the approximate values $\psi = 35°$ and $\psi = 145°$.

If the satellite is considered to be a “sphere” a simple model is built by mediating the value of acceleration for the angle ψ between the satellite, the Earth and the Sun. Thus, the acceleration can be calculated using the formula:

$$f_{\bar{r}} = \frac{A}{M}\frac{E}{c}C_{sferă} \tag{3.21}$$

where C_{ball} is a constant determined numerically, which the average size and optical properties of GPS satellites.

Tab. 3.2 GPS satellites parameters (ball type satellites)

GPS satellite type	Ratio Aria/Mass [m^2/Kg]	$C_{sferă}$
Block I	0,01513	0,8876
Block II	0,01667	0,8551
Block IIR	0,01606	0,8134

The major semi–axis variation graphs, designed for 50 and 500 hours show that it has two types of perturbations, a short-periodic one, and long-periodic one. The short-periodic perturbation has a period equal to the orbital period (12 hours), and a variation of 1 km, while the long-periodic perturbation has a period of 240 hours.

The eccentricity has a secular perturbation superimposed on a short-periodic perturbation with period of 6 hours, with the order of magnitude $1,5 \cdot 10^{-8}$.

The inclination has two types of disturbances, a short-periodic and secular one. Short-periodic disturbance period is equal to the orbital period (12 hours) and a variation of degree.

The perigee argument undergoes mixed periodic perturbation:

- a short periodic perturbation with a 6 – hour period, and an amplitude of $1 \cdot 10^{2}$ degrees
- a short periodic perturbation with a 6- hour period, and an amplitude of $3 \cdot 10^{2}$ degrees
- a secular perturbation

The longitude of the ascending node suffers mixed periodic perturbation:

- a short periodic perturbation with a 6- hour period, and an amplitude of $4 \cdot 10^{-3}$ degrees
- a secular perturbation

3.5.3 The anisotropic thermal emission

The anisotropic thermal acceleration has a linear variation depending on the temperature variation of two parts of the satellite body, and on the ratio of effective sectional area and mass of the satellite. The acceleration due to anisotropic thermal emission, for a temperature difference "at day time" is of order 10^{-13} Km/s^2.

The major semi–axis undergoes perturbations equal to the orbital period, and to amplitude $4 \cdot 10^{-5}$ kilometers.

Eccentricity undergoes a short periodic perturbation of a 6 – hour period, and amplitude $6 \cdot 10^{-10}$ superimposed on a secular perturbation.

The inclination of the orbit undergoes a short periodic perturbation of a period equal to the orbital period, and of amplitude and $3 \cdot 10^{-8}$

The longitude of the ascending node undergoes a mixed periodic disturbance:

- short-periodic perturbations with a 3 – hours period, and amplitude $1 \cdot 10^{-7}$ degrees
- long-periodic perturbations with a 24 – hours period.

3.5.4 The acceleration produced by antennas emissions

The emission of the navigation antennas of the GPS satellites produces a constant radial acceleration, and as a consequence, there is a change of acceleration in this direction.

The GPS satellites provide a continuous emission, with an output of 70 to 80 watts in the direction of the antenna when emitting on the two fundamental frequencies L1 and L2.

The force expressed in newtons due to photon absorption from a flux of incident radiation *(E)* is given by:

$$F = \frac{E}{c} \tag{3.22}$$

Considering an emission power of 80 watts of the antennas, the resultant acceleration on different types of GPS satellites is:

Block I: 5.3x10-10 m/s2

Block II: 3.0x10-10 m/s2

Block IIR: 2.4 x10-10 m/s2

The major semi–axis undergoes more short-periodic perturbations:

- a short periodic perturbation with a period equal to the orbital period, and amplitude $4 \cdot 10^{-5}$ kilometers;
- a short periodic perturbation with a 3 hour period, and amplitude of $1 \cdot 10^{-5}$ kilometers

The eccentricity has a short periodic disturbance with a 3 hours period and an amplitude of $2 \cdot 10^{-10}$ superposed on secular perturbation.

The inclination has several periodic perturbations:

- a short periodic perturbation with a period equal to the orbital period, and amplitude $3 \cdot 10^{-8}$ degrees.
- a mixed periodic perturbation superposed on a short periodic disturbance.

The perturbations acting on the longitude of the ascending node are mixed periodical, with periods of 3, 6, 18 and 48 hours, and with amplitudes of $2 \cdot 10^{-8}$ and $1{,}2 \cdot 10^{-7}$ degrees.

3.5.5 The elipses

Eclipse modeling region

The method is based on the tests which determine if the lines from the edges of the Sun to the Earth crosses or not the satellite. If a junction is made and the distance from the Sun at this point is less than the distance sun-satellite, the satellite is in the penumbra or umbra.

An immediate plan is defined in the center of the earth, is the vector of the Earth-Sun and Earth-satellite array. In this two-dimensional space, the Sun is represented as a circle. In plan, the light rays leaving at the edges of the sun and is tangent to the Earth Sun and the Earth determines the edge of the penumbra and umbra.

Determination of the intersection points is performed using the mathematical ellipsoid approximation for the Earth:

$$\frac{x^2 + y^2}{p^2} + \frac{z^2}{q^2} = 1 \tag{3.23}$$

where *x*, *y*, *z* are coordinates of a point on the ellipsoid, p is the equatorial radius and q is the polar radiu.

Equation that connects the satellite with one of the edges of the Sun is:

$$\begin{pmatrix} x \\ y \\ z \end{pmatrix} = \begin{pmatrix} a_1 \\ a_2 \\ a_3 \end{pmatrix} + \lambda \begin{pmatrix} b_1 \\ b_2 \\ b_3 \end{pmatrix} \tag{3.24}$$

where (a_1, a_2, a_3) are coordinates of the position vector of the satellite and (b_1, b_2, b_3) are coordinates of the position vector of an edge of the sun. Thus the above equation (3.24) can be written as:

$$\frac{x-a_1}{b_1-a_1}=\frac{y-a_2}{b_2-a_2}=\frac{z-a_3}{b_3-a_3} \tag{3.25}$$

The vectors $\vec{a}$ and $\vec{b}$ can be obtained for a specific period from the precise ephemeris or from numerical integration. From equation (3.25), y and z can be written as a function of x and the coefficients $\vec{a}$ and $\vec{b}$.

$$y=\frac{x(b_2-a_2)+a_2b_1-a_1b_2}{b_1-a_1} \qquad z=\frac{x(b_3-a_3)+a_3b_1-a_1b_3}{b_1-a_1} \tag{3.26}$$

Developing is obtained a 2nd degree equation of the form:

$$Ax^2+Bx+C=0$$

with the coefficients:

$$A=q^2\left[(b_1-a_1)^2+(b_2-a_2)^2\right]+p^2(b_3-a_3)^2$$

$$B=2q^2(b_1b_2a_2-a_1b_2^2-a_2^2b_1+a_1a_2b_2)+2p^2(b_1b_3a_3-a_1b_3^2-a_3^2b_1+a_1a_3b_3)$$

$$C=q^2\left(b_1a_2-b_2a_1\right)^2+p^2\left(b_1a_3-b_3a_1\right)^2-p^2q^2(b_1-a_1)^2$$

To solve the system is necessary to know the coordinates of the edges of the Sun. Real solutions of the 2nd degree equation is the x coordinates of the points of intersection of the line that goes from one edge of the Sun and satellite with the ellipsoid.

The existing condition for real solutions is:

$$B^2-4AC\geq 0\,.$$

Author the method proposed by consists in using the line that passes through the center of the sun points - TV. Sun center coordinates can be obtained either by numerical integration or from the specialized sites. For this study the author used data from www.imcce.fr site / en / ephemerides. This site provides the geocentric coordinates of the Sun based on astronomical unit. For the study made by the author have been used sun coordinates obtained by numerical integration.

Below are presented the situations of intersection of the straight line passing through the points and center of the Sun-satellite Earth ellipsoid.

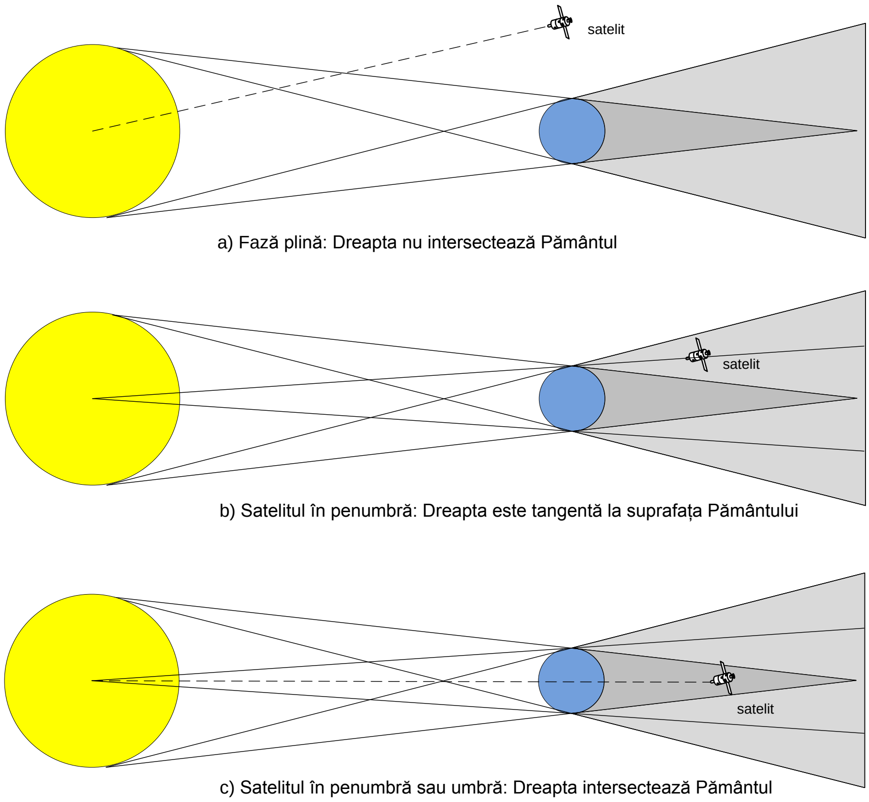

Fig. 3.1 Determination of GPS satellite position. The solution proposed by the author

- If the system has no real solutions when the satellite is fully illuminated.
- If the system has only one real solution, then right is tangent to the ellipsoid and the satellite may lie in the penumbra or completely illuminated. Then it is necessary to determine and y and z coordinates of the intersection to calculate the distance to the Sun. If the distance is greater than the distance between the sun and the satellite, the satellite is fully illuminated, the satellite failing in the penumbra area.
- If the system has two real solutions, it is necessary to determine and y and z coordinates of the intersection to calculate the distance to the Sun.
- If the distance is greater than the distance between the sun and the satellite, the satellite is fully illuminated, otherwise satellite is in the penumbra or umbra.

For this study, the author determined the coordinates of the Sun by numerical integration every minute for 365-days using the start date, date 10.02.2011, time: 00:00:00 UTC.

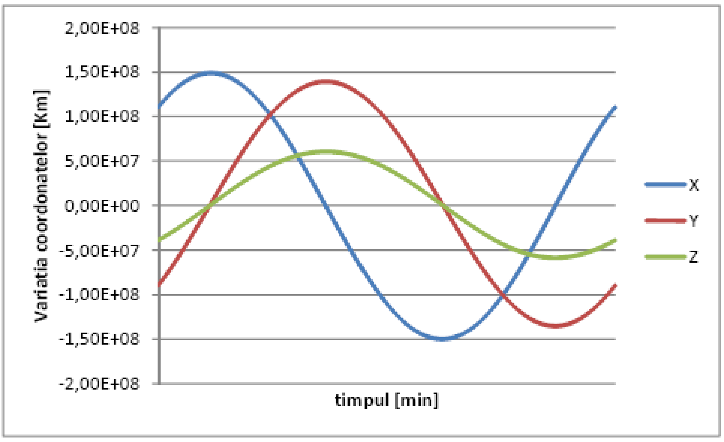

The coordinates variation of the Sun for a year

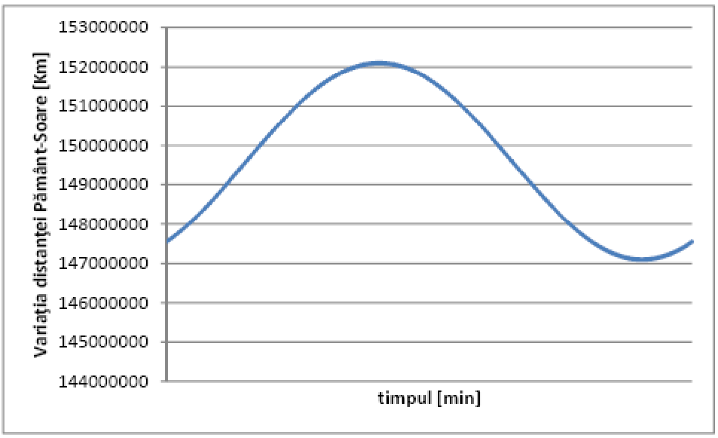

The variation of the radius vector of the sun for a year

For determining the geocentric coordinates of the satellite every minute for a period of 365 days author started from the initial conditions since 10.02.2011 00.00 UT:

xai = 2425.8676; vxai = 3.8327;
yai = -15215.1157; vyai = 0.4529;
zai = 21743.2188; vzai = -0.1055;

Tab. 3.3 The number of GPS satellite solutions entering in the umbra

The ellipsoid type	Number of real solutions of the system depending on perturbation		Number of minutes for the satellite in the umbra or penumbra	
	J2	Direct solar radiation pressure	J2	Direct solar radiation pressure
p = 6378,137 Km q = 6356,752 Km	26424	26278	0	0
p =q = 6378,137 Km	26506	26376	0	0
p =q = 6402 Km	26702	26488	0	0

For all cases the system was real solutions revealed that the satellite did not go to any time in the Earth's umbra or penumbra.

The numerical results concerning the satellite crossing through the penumbra and umbra of the earth are in line with the actual movement of satellites. Thus, the observations made on the satellites is known that the time spent by them in eclipse is only 1-2 minutes.

3.5.6 The Poynting – Robertson effect

The Poynting-Robertson effect, named after John Henry Poynting and Howard Percy Robertson, braking is a process whereby solar radiation causes dust particles in the solar system to spin on a downward spiral. The braking force is produced basically by the tangential component of the force caused by the radiation pressure on the movement of the dust particles.

For proper dust surrounding the Sun's radiation sun appears to be coming a little forward direction (aberration of light). As a result, the absorption of of this radiation lead to a force component against the direction of movement. The angle of aberration is extremely small, because the radiation travels at the speed of light as particles of dust is moving with a speed order of magnitude required is much lower.

The braking force produced by the The Poynting-Robertson effect can be understood as a force acting in the direction opposite to the direction of motion of the dust particle's own orbit, which produces a decreasing effect of angular momentum. Thus, while the dust particle moving on a spiral slowly towards the Sun, its orbital speed increases continuously.

The Poynting-Robertson force is equal to:

$$F_{PR} = \frac{Wv}{c^2} = \frac{r^2}{4c^2}\sqrt{\frac{GM_S L_S^2}{R^5}} \tag{3.27}$$

where:

W - is the power of incident radiation,,

v - is the velocity of the powder particles,

c - the speed of light,

r - is the radius of the object,

G - the gravitational constant of the universe,

M_s - the mass of the Sun,

L_s - solar brightness

R - is the radius of the orbit on moving object.

Solar brightness $L_\odot$ represents the radiant flux (power emitted as photons) to measure the brightness of stars. A solar brightness unit is equal to the current brightness accepted by Sun and has a value of 3.839 x 10^{26} W, or 3.839 x 10^{33} erg/s.

Solar brightness refers to the measured solar irradiance on the Earth or by the satellites orbiting the Earth. The average irradiance at the top of Earth's atmosphere is sometimes known as the solar constant, $I_\odot$. Irradiation is defined as the power per unit surface area, so that the solar luminosity (total energy emitted by the sun) is the irradiance received on the Earth (the solar constant) multiplied by the surface of the sphere whose radius is the average distance between Earth and the Sun:

$$L_S = 4\pi k A^2 \tag{3.28}$$

where:

A - is the astronomical unit in meters

k - is a constant (whose value is very close to one) that reflects the fact that the average distance from Earth to the Sun is not exactly one astronomical unit.

considering:

c = 299792458m/s

r = 1m

G = 6,674*10^{-11} m^3/Kgs^2

M_s = 2*10^{30} Kg

L_s = 3,9*10^{26} Kgm^2/s^3

R = 150000000000 m (astronomical unit)

The result is a Poynting-Robertson force value of:

$$F_{PR} = 1{,}4 \cdot 10^{-12}\ kN$$

The Poynting-Robertson acceleration is determined from the ratio of the Poynting-Robertson force and mass of the satellite.

$$a_{PR} = \frac{Wv}{c^2 m} = \frac{r^2}{4c^2 m}\sqrt{\frac{GM_S L_S^2}{R^5}} \tag{3.29}$$

Considering the ratio $\frac{r^2}{m}$ between the radius of the satellite and its mass as a ratio Area / Mass particular satellite, the The Poynting-Robertson acceleration has the value:

GPS satellite type	Ratio Area/Mass [m^2/Kg]	The Poynting-Robertson acceleration [Km/s]
Block I	0,01513	$6,930 * 10^{-15}$
Block II	0,01667	$7,635 * 10^{-15}$
Block IIR	0,01606	$7,356 * 10^{-15}$

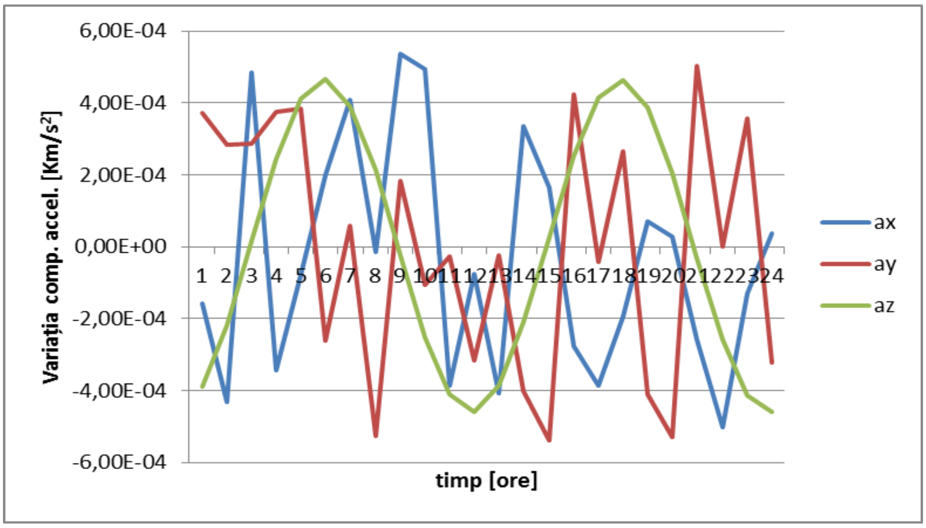

The variation of acceleration components due to The Poynting-Robertson effect

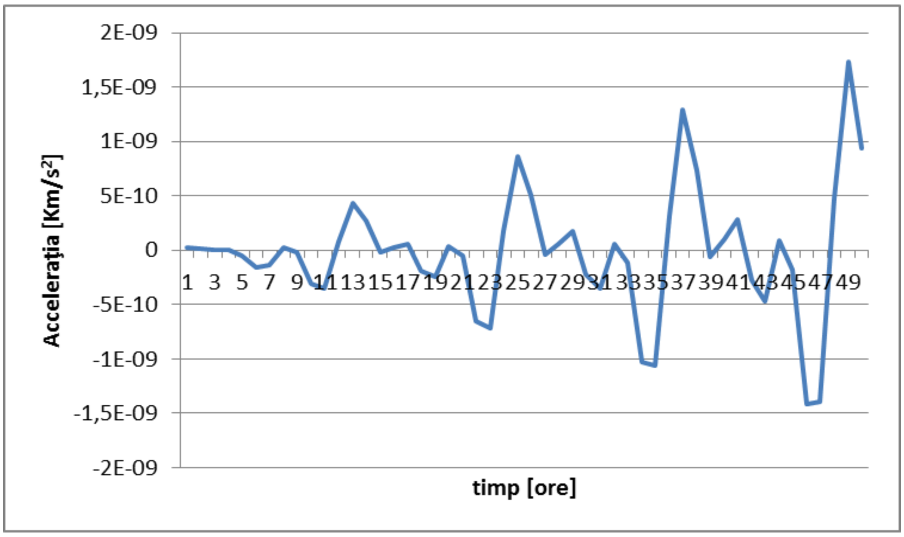

The variation of total acceleration due to The Poynting-Robertson effect

From the graphs of variation of the orbital elements $(a, \ e, \ i, \ \omega, \ \Omega, \ M)$, the radius vector and the speed of the TSC system, for a period of 50 hours, a GPS satellite follows:

- semi-major axis suffer perturbations with amplitude of 1 cm.
- eccentricity present a secular perturbation superimposed over on a short-periodic perturbation with a period of 4 hours and an order of magnitude of 10^{-10} Km.
- inclination is very stable, this presenting very small variations with order of 10^{-9} degrees.

4. QUALITY ANALYSIS OF GPS SATELLITE MOVEMENT

4.1. Introductory notes

Before the French mathematician Henri Poincare, studies on the dynamical systems were focused on finding solutions for explaining functions in solving the equations of motion. The dynamical systems theory has undergone a significant evolution in the late nineteenth century by the contribution made by the French mathematician Henri Poincare. Poincare thinks of the possibility to solve the geometry of the solutions without developing any formulas. Thus, qualitative properties of the solution are found without knowing its exact formula. This new method has helped solving many problems involving differential equations.

Qualitative or geometrical analysis deals with the analysis of the evolution of dynamic systems solutions. This analysis is done in phase space, which is the state space, i.e. the space where all sizes are represented graphically describing the system state. In the phase space, a dynamic state, at a certain time is described graphically by a point, defined by a set of phase variables, i.e. a set of minimum variables that describe completely the system state. Changing the system state in relation with time is a trajectory in the phase space. The collection of all possible trajectories (local or global) of a dynamical system is called the phase portrait (local or global).

We analyze in terms of quality movement of a particle (satellite, comet) around the central body in a variety of fields, under the influence of zonal harmonics up to the 6th order, on any type of orbit, and for different values of the energy system.

The gravitational field in which the potential is given by:

$$V(r) = \frac{A}{r} + \frac{B}{r^3} \tag{4.1}$$

is called Schwarzschild problem, while the field in which the potential is given by the relation:

$$V(r) = \frac{A}{r} + \frac{B}{r^2} \tag{4.2}$$

is named Manev type field.

4.2 Qualitative analysis of GPS satellite motion under the influence of zonal harmonics of higher order

The gravitational potential up to the sixth zonal harmonic is:

$$V(r) = \frac{\mu}{r} - \frac{\mu}{r} \cdot \sum_{n=2}^{6} \left(\frac{a_{ec}}{r} \right)^n \cdot J_n \cdot P_n(\sin\varphi) \tag{4.4}$$

To make calculation less difficult, we can note:

$$a_1 = \mu \ , \ a_2 = 0 \ \text{și} \ a_k = -\mu \cdot a_{ec}^{k-1} \cdot J_{k-1} \cdot P_{k-1}(\sin\varphi) \quad pentru \quad k = 3..6 \tag{4.5}$$

resulting in the new form of gravitational potential:

$$V(r) = \sum_{n=1}^{7} \frac{a_n}{r^n} \tag{4.6}$$

In order to describe the movement of the two bodies, satellite-central body (particle-center) which goes on in a plane, we choose the coordinates configuration - impulse.

The position of the satellite will be defined by the vector,

$$q = (q_1, q_2) \in \Re^2 \setminus \{(0,0)\}, \tag{4.7}$$

and the velocity will be defined by the impulse vector.

$$p=(p_1,p_2)\in\Re^2, \qquad p=\dot{q}\,. \tag{4.8}$$

The configuration (position) vector is not defined in the origin because this is point is associated with a singularity of the system (particle collision - center).

To remove singularities and regularize the equations of motion we use the McGehee transformations of second order. The equations of motion become:

$$\begin{aligned} r' &= \frac{dr}{ds} = r\cdot x \\ \theta' &= \frac{d\theta}{ds} = y \\ x' &= \frac{dx}{ds} = \frac{7}{2}x^2 + y^2 - \sum_{n=1}^{7} n\cdot a_n\cdot r^{7-n} \\ y' &= \frac{dy}{ds} = \frac{5}{2}\cdot x\cdot y \end{aligned} \tag{4.9}$$

The prime integrals become:

$$\begin{aligned} x^2+y^2 &= h\cdot r^7 + 2\sum_{n=1}^{7} a_n\cdot r^{7-n} \\ y^2 &= C^2\cdot r^5 \end{aligned} \tag{4.10}$$

At this point both the equations of motion, and the prime integrals are well defined for limit r $\to$ 0, so the phases space can be analytically extended to contain the variety $\{(r,\theta,x,y)\,|\,r=0\}$ as well.

Variety $M_0=\{(r,\theta,x,y)\,|\,r=0,\ \ \theta\in S^1,(x,y)\in\Re^2\}$ is defined, where S^1 is the interval $[0, 2\pi\ ]$ with mistaken heads and variety of constant energy

$$.\ M_h=\{(r,\theta,x,y)\,|\,x^2+y^2=h\cdot r^7+2\sum_{n=1}^{7}a_n\cdot r^{7-n},\ \ \theta\in S^1,(x,y)\in\Re^2\}\,.$$

Variety of collision will be the intersection of the two varieties defined above, ie:

$$M_{col}=\{(r,\theta,x,y)\,|\,r=0,\ \ x^2+y^2=2\cdot a_7,\ \ \theta\in S^1,(x,y)\in\Re^2\} \tag{4.11}$$

The expression of angular momentum of the integral in polar coordinates shows that if $r\to 0$ then $\theta'\to\infty$. In terms of physical motion, the particle moves on the orbits, in spiral, around the center of an infinite number of times, until collision happens (or, after ejection). This is the black hole effect (Diacu et al., 1995). From the energy integral expression we can see that the escape $r\to\infty$ is possible only for the negative energy $h\geq 0$.

Since the variable θ does not appear explicitly in the equations of motion, or prime integrals the four-dimensional space (r,θ,x,y) can be reduced to the three dimensional space (r,x,y) by factoring the current through S^1. Any solution within the space (r,x,y) should be regarded as a variety of solutions in four-dimensional phase space. Using the first integral of angular momentum, reduce to two-dimensional phase space (r,x) . Vector field is:

$$\begin{aligned} r' &= r\cdot x \\ x' &= \frac{7}{2}\cdot h\cdot r^7 - \frac{5}{2}\cdot C^2\cdot r^5 + \sum_{n=1}^{6}(7-n)\cdot a_n\cdot r^{7-n} \end{aligned} \tag{4.12}$$

where the integral of energy is used for taking *x* out the second ecuation

$$x^2 = h\cdot r^7 - C^2\cdot r^5 + 2\cdot\sum_{n=1}^{7} a_n\cdot r^{7-n} \tag{4.13}$$

The tor M_{col} was reduced to circle $\{(r,x,y)\,|\,r=0; x^2+y^2=2\cdot a_7\}$ within the three-dimensional space, while within the two-dimensional space it was reduced to two points $N(r=0, x=\sqrt{2a_7})$ and $P(r=0, x=-\sqrt{2a_7})$.

For the preparation of the phase portraits of GPS satellite motion around the central body the graphic of function $x(r) = \pm\sqrt{f(r)}$ will be analyzed where $f(r) = h \cdot r^7 - C^2 \cdot r^5 + 2 \cdot \sum_{n=1}^{7} a_n \cdot r^{7-n}$ also the values of the coefficients in the equations of motion and equations solutions $f(r) = 0$ and $\frac{df(r)}{dr} = 0$ will be taken into account.

The most general case will be considered, when the derivative $f'(r)$ has 5 sign changes (the maximum) for the of case negative energy; there results that, according to Descartes' rule, for the collisional case $a_7 > 0$ the equation $f(r) = 0$ has 5 positive roots, and for the non-collisional case $a_7 < 0$, the equation has four positive roots . When the energy is positive or null we assume that the derivative $f'(r)$

has 4 sign changes (the maximum), so, according to the same Descartes rule the equation $f(r) = 0$ will have 5 positive roots for $a_7 > 0$ and 4 positive roots for $a_7 < 0$. .

There is a critical value of the energy that will determine, together with the sign of the coefficient function $f(r)$ different configurations for the phase portraits.

Case $a_7 > 0$, $h < h_c < 0$

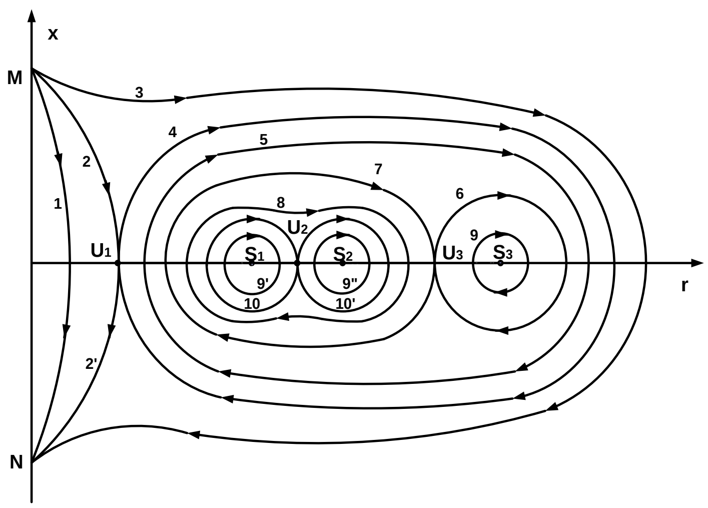

The explanation of the given phase portrait is:

S - stable equilibrium point (center), which represents stable circular motion;
U - unstable equilibrium point (source), which represents unstable circular motion;
(1) and (3) - heterocline orbits, spiraling movement of ejection type - collision;
(2) and (2 ') represents motion on the spiral orbits that start from collision, and tend to asymptotical unstable form, or vice versa;
(4), (6), (7), (10) and (10 ') – homocline trajectory, which in physical terms is a spiral orbit which starts asymptotically from an unstable circle, and tends asymptotically to the same unstable circle;
(5), (8) and (9), (9 '), (9 '') – stable periodical or cvasi-periodical orbits, with eccentricity that decreases from (5) which has significant values, up to (9') and (9 '). Nothing can be mentioned about the eccentricity of orbits (9);

4.3 Practical application – The GPS SATELLITE

Replace in the function expression,

$$f(r) = h \cdot r^7 - C^2 \cdot r^5 + 2 \cdot \sum_{n=1}^{7} a_n \cdot r^{7-n} \tag{4.14}$$

all coefficients with known parameters of the Earth:
- the zonal harmonics J2 to J6 on
- the legendary polynomials for null latitude
- the gravitational constant (μ)
- the energy calculated by the formula $h = -\dfrac{\mu}{a}$
- the angular momentum of the relationship $C^2 = \mu \cdot a \cdot \left(1 - e^2\right)$
- the major semi-axis of the geostationary satellite a = 26559.4 km

After solving the equation $f(r) = 0$ the following solutions result $r_1 = 26329{,}11$ and $r_2 = 26788{,}02$; after solving the equation $f'(r) = 0$, the following solution results $r_1' = 26563{,}5$ which is exactly the major semi-axis of the geo – stationary satellite.

There result the graphs of the functions $x(r) = \pm\sqrt{f(r)}$ and after that the phase portrait using the program Maple 14.

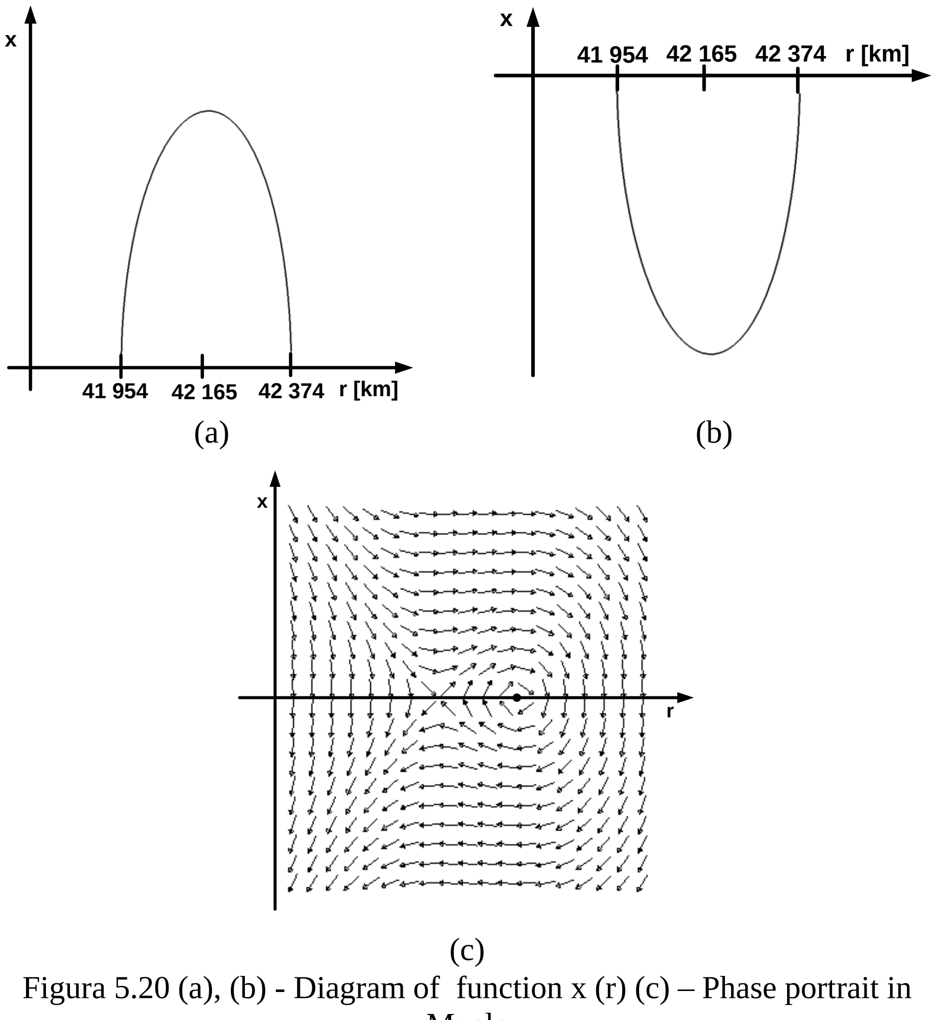

Figura 5.20 (a), (b) - Diagram of function x (r) (c) – Phase portrait in Maple

In the following the explicit phase portrait is explained. The GPS satellite position is marked by the point (S), which means stable circular motion at distance *r* off the central body

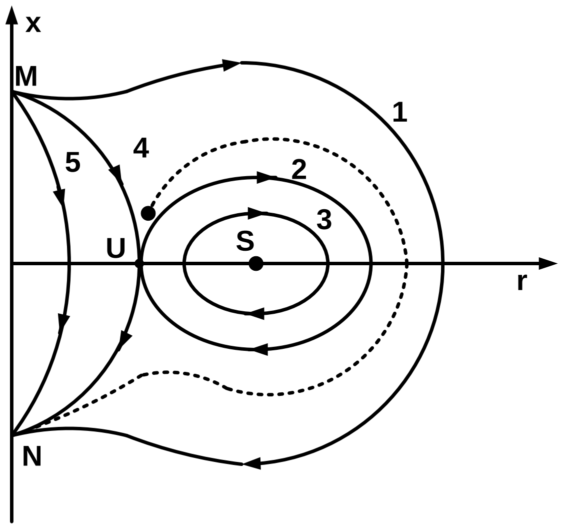

Figure 5.21 The explicit phase portrait of the GPS satellite movement

GPS satellite orbit is stable as long as r is between the values $r_1 = 26329{,}11$ and $r_2 = 26788{,}02$. If in its movement on the orbit the GPS satellite exceeds the value of r_2 to the right, or the value of r_1, to the left, there results the spiral physical movement along an orbit which tends asymptotically to collision. The dotted line represents the fictitious trajectory of a geostationary satellite that is leaving the orbit and moves in an elliptical orbit with increasing eccentricity, tending asymptotically to collision.

4.4 Conclusions for the qualitative analysis

This chapter presents a new approach to the theory of dynamical systems in general, and of the celestial mechanics, in particular, through the qualitative method, whose initiator is Poincare. The motion of a particle (satellite, comet) around the central body in various field types was observed: Schwarzschild, Manev, under the influence of zonal harmonics up to degree 6.

From the above mentioned it is important to observe the utility of McGehee transformations, that are designed to eliminate singularities, and regularized equations of motion. Transformations made it possible to replace collision t with a limited variety, attached to the phase space. The McGehee transformations allow the study of movement near collision.

In this chapter we noted that collisions can also occur when $C \neq 0$. Therefore, when $r \to 0$ there results that $\theta' \to \infty$, i.e. the particle executes a spiral motion of an infinite number of times around the center, up to collision or after ejection, which is the effect of the black hole (Diacu et al., 1995).

If the system's energy is negative (h <0) the particle can not escape. If the maximum coefficient (a7 <0) is negative, the movement is executed without collision.

From the presented situations we can derive that: there are several types of orbits:

- bounded and collisional, which start from ejection, reach a maximum distance, or an unstable equilibrum, and come back to collision;
- bounded and non-collisional, which can be:
    - stable or unstable circulars

- regular (including librations, radials) and quasi-periodicals
- homocline, starting from an unstable equilibrium and return to it
- heterocline that connect two points of unstable equilibrium

- boundless and collisional, i.e. as ejection – escape and infinity - collision;
- not bounded and non-collisional, coming from infinity, reach a minimum distance or a point of unstable equilibrium and return to infinity.

5. CONCLUSIONS

Finally an overview of the notions and analyzes performed in this paper is made, highlighting significant and original results.

In order of the chapters, will summarizing the important parts from each section of this paper and the conclusions drawn.

Chap. I. Description of NAVSTAR/GPS satellite system, identification of GPS technology applications, description of reference systems and time scales required for study of disturbing forces acting on GPS satellites.

Chap. II. Quantitative analysis of GPS satellite motion under the influence of gravitational and non-gravitational perturbations type.

Chap. III. Quantitative analysis of non-gravitational perturbations type: direct solar radiation pressure, indirect solar radiation pressure, anisotropic thermal emission, the antennas emission and empirical models of the solar radiation pressure.

Chap. IV. Analysis of perturbed motion of satellites NAVSTAR / GPS based on numerical method using 4th order Runge-Kutta integration algorithm. The advantages of this integration algorithm are stability and easy modeling perturbed motion equations for GPS satellite. Algorithm is slowly, the computing time increasing considerably for long periods of time, which is the main disadvantage of the algorithm. Calculation program is developed by the author in the C ++ programming language, in a simple manner, but providing information for the analysis of GPS satellite motion.

4.4 Starting from the initial conditions (position and velocity) for GPS satellite of study for 10.02.2011 00.00 UT were presented graphs of variation of the gravitational acceleration components given by gravitational perturbations J_2, J_3, J_4, J_5, J_6, gravitational attraction of the Sun and Moon, relativistic effects and Poynting-Robertson effect for an orbital period and the total accelerations graphs of variation of these gravitational perturbations for a period of 50 hours. Are determined average values of the total accelerations, unit being Km/s2.

4.5 It is observed that the gravitational perturbations have the greatest influence among them highlighting zonal harmonic J2 of which order of magnitude is $2x10^{-7}$ Km/s^2. Between the non-gravitational perturbations, the direct solar radiation pressure has the greatest effect with the order of magnitude of 4.4×10^{-10} Km/s^2, while the order of magnitude of the Poynting-Robertson effect is 6.9×10^{-15} km/s^2.

4.6 Are determined the effects of non-gravitational perturbations on the keplerian orbital elements.

4.6.1 As a result of action of direct solar radiation pressure on a GPS satellite has revealed the following effects:

- Semi-major axis shows a short-periodic perturbation with a 6 hours period superimposed on a secular perturbation. For an orbital period, semi-major axis suffers a variation of 4 meters.

- Eccentricity present a secular perturbation superimposed on a short-periodic perturbation with a 6 hours period having the order of magnitude of $4,8 \cdot 10^{-8}$ Km.

- Inclination present same type of perturbation as semi-major axis, a short-periodic perturbation superimposed on a secular perturbation. Short-period perturbation have the period of 6 hours and the order of magnitude is $3 \cdot 10^{-6}$ degrees.

- Longitude of ascending node suffers a short periodic perturbation with a period of 6 hours and an amplitude of $1,7 \cdot 10^{-6}$ degrees, superimposed on a secular perturbation.

4.6.2 Based on the models of the Earth's radiation, reflected and emitted radiation, the irradiance graphs has been made for different values of albedo Earth and the ψ angle – angle between Satellite-Earth-Sun. Based on the reflectivity and emissivity data of the Earth supplied by CERES for the period from February to June 2011 has been made the graphics of these variation and has been determined the mean values.

Using the least squares method we determined the reflectivity and emissivity coefficients for the period February to June 2011, for the case when them are write like harmonic development according to the latitude. There have been determined the variation graphs of radial and tangential components of acceleration due to reflected and emitted radiation from Earth to GPS satellites (satellite P07 in particular), where satellites are modeled as "box-wing".

If the GPS satellite is considered having the form of "sphere" have been determined the graphs of variation of the keplerian elements for 50 and 500 hours resulting in the following effects:

- Semi-major axis present two types of perturbations, one short and one long-periodic. Short-periodic perturbation is equal to the orbital period (12 hours) and a variance of 1 km, and the long-periodic perturbation have period of 240 hours.

- Eccentricity present a secular perturbation superimposed on a short-periodic perturbation with period of 6 hours having the order of magnitude of $7 \cdot 10^{-6}$ Km.

- Inclination presents two types of perturbations, one short-periodic and one secular perturbation. Short-periodic perturbation is equal to the orbital period (12 hours) and with a variance of $7 \cdot 10^{-6}$ degrees.

- Mean anomaly suffer a short periodic perturbation having a 6 hours period superimposed on secular perturbation.

- Argument of perigee suffer a mixed periodic perturbations:

a short periodic perturbation having a period of 6 hours and an amplitude of $1 \cdot 10^{-2}$ degrees

a short periodic perturbation having a period of 6 hours and an amplitude of $3 \cdot 10^{-2}$ degrees

a secular perturbation

- Longitude of ascending node suffer a mixed periodic perturbations:

a short periodic perturbation having a period of 6 hours and an amplitude of $4 \cdot 10^{-3}$ degrees

a secular perturbation

4.6.3 Due to anisotropic thermal emmission upon a GPS satellite the following effects were revealed:

- The semimajor axis and inclination do not suffer perturbations

- The eccentricity has a short periodic perturbation equal to the orbital period and an amplitude of $8 \cdot 10^{-10}$

- The mean anomaly suffers short periodic perturbations with a period of 6 hours superimposed over a secular perturbation.

- The perigee argument suffers short periodic perturbations with a period of 6 hours superimposed over a secular perturbation.

- The longitude of ascending node suffers a long periodic perturbation having an amplitude of $2 \cdot 10^{-11}$ degrees.

4.6.4 Due to GPS navigation antennas emission the following effects were revealed:

- The semimajor axis and do not suffer perturbations

- The eccentricity has a short periodic perturbation equal to the orbital period and an amplitude of $8 \cdot 10^{-10}$

- The perigee argument suffers short periodic perturbations with a period of 6 hours

- Argumentul perigeului suferă perturbații scurt periodice având perioada de 6 ore.

- The longitude of ascending node suffers a long periodic perturbation having an amplitude of $1 \cdot 10^{-8}$ degrees.

4.6.5 Based on studies carried out by Adhya - 2005 regarding the GPS satellites eclipses, we developed a mathematical model to determine the period of time during which the GPS satellite enters in Earth's penumbra or umbra. We consider cases where GPS satellite is perturbed by direct solar radiation pressure or J_2 and I developed the solutions of the mathematical model. For all cases, the system has real solutions revealed that the satellite did not go to any time in the Earth's umbra or penumbra.

At theoretical modeling of the penumbra region through which a GPS satellite passing, revealed that the satellite at a speed of about 3.86 km/s crossing this area is performed within a period 15.3 minutes.

4.6.6 As a result of Poynting-Robertson effect on a GPS satellite has revealed the following effects:

- Semi-major axis suffers perturbations with maximum amplitude of 1 cm.

- Eccentricity present a secular perturbation superimposed over a short-periodic perturbation with a period of 4 hours and a magnitude order of $1,5 \cdot 10^{-11}$

- Inclination is very stable, presenting short periodic perturbations with a period of 4 hours and a magnitude order of $1 \cdot 10^{-8}$ degrees.

- The other orbital elements suffer short periodic perturbations with a period of 6 hours and an amplitude of $8 \cdot 10^{-7}$ degrees.

Chap. V Presents a new approach to the theory of dynamical systems in general and celestial mechanics in particular by using qualitative method whose initiator is Poincare. It was considered the motion of a particle (satellite) around the central body in different field types: Schwarzschild, Manev and under the influence of zonal harmonics up to grade 6. It was analyzed the GPS satellite motion on any type of orbit and for different values of energy of the system.

5.2 It notes the usefulness of McGehee transformations that are designed to eliminate singularities and to regularize the equations of motion. Through changes was made to explode the variety of collision and it was replaced a variety limit attached to space phases. McGehee transformations act as a lens with a infinite power magnification on a collision singularity, thus allowing the study of motion near collision.

5.3 It was made a practical application for GPS satellite. The GPS satellite orbit is stable as long as r is between values $r_1 = 26329,11$ and $r_2 = 26788,02$. If the movement of a GPS satellites on an orbit exceeds at right the value of r_2 or at left the value of r_1, the resulting physical movement is a spiral orbit which tends asymptotically to the collision. Such that, qualitative results are confirmed by numerical results.

REFERENCES

1. Aksnes, K., „*Short-period and long-period perturbations of a spherical satellite due to direct solar radiation*", Celestial Mech. 1976
2. Anselmo, L. et al., „*Orbital perturbations due to radiation pressure for a spacecraft of complex shape*" Celestial Mech. 1983
3. Anselmo, L. et al., „*Modelling of orbital perturbations due to radiation pressure for high Earth satellites in ESA Spacecraft Flight Dynamic*", ESA SP-160, 1981
4. Arnold, V. I., „*Geometrical Methods in the Theory of Ordinary Differential Equations*", Berlin: Springer 1983
5. Arnold V., Kozlov V., Neishtadt A., "*Mathematical aspects of classical and celestial mechanics*", Springer, Germania, 2006
6. Barlier, F. et al., „*Non-gravitational perturbations on the semimajor axis of LAGEOS*", Ann. Geophys., 1986
7. Bar-Sever Y. and Kuang D., "*New Empirically Derived Solar Radiation Pressure Model for Global Positioning System Satellites*", IPN Progress Report 42-159, 2004
8. Barrar, R., "*Some remarks on the motion of a satellite of an oblate planet*", The Astronomical Journal, vol.66, 1961
9. Barrie W.J., "*Discovering the solar system*", Marea Britanie, 2007
10. Batrakov, I.V., "*Dynamics of Sattelites*", IUTAM Symposium, Paris 1962, Springer-Verlag, Berlin, 1963
11. Bertotti, B., Farinella, P., "*Physics of the Earth and the Solar System*", Kluwer Academic Publishers, 1990
12. Beutler G., "*Methods of celestial mechanics*", vol. 1 și 2, Springer, Germania, 2005
13. Born, G., „*Motion of a Satellite under the influence of an oblate Earth*", 2001
14. Broucke, R.A., "*Numerical integration of periodic orbits in the main problem of artificial satellites*", Celestial Mechanics and Dynamical Astronomy, 1994
15. Brouwer, D., "*Solution of the problem of artificial satellite theory without drag*", the Astronomical Journal, vol.64, 1959
16. Brouwer, D., Clemence, G.M., "*Methods of Celestial Mechanics*", Academic Press, New York and London, 1961
17. Burns, A.J., "*Elementary Derivation of the Perturbation Equations of Celestial Mechanics*", American Journal of Physics, 1976
18. Capitaine, N., "*Systèmes de références spatio-temporelles*", Romanian Astronomical Journal, Bucureşti, 2002
19. Christoiu A., Murray C. D., „*A second order Laplace-Lagrange theory applied to the uranian satellite system*", 1997
20. Claessens, S.J., Featherstone, W.E., „*Computation of geopotential coefficients from gravity anomalies on the ellipsoid*", Western Australian Centre for Geodesy, 2004
21. Collins G., „*The foundations of Celestial Mechanics*", SUA, 2004
22. Cojocaru, S., „*Sistemul global de poziţionare GPS/GLONASS – prezent şi viitor* ", Zilele Academiei Clujene, Cluj-Napoca 1996
23. Cojocaru, S., „*Contribuţii la studiul erorilor orbitale ale sateliţilor GPS pe seama potenţialului gravitaţional terestru*", Teză de doctorat, Institutul Astronomic, Bucureşti, 1997
24. Cojocaru, S., „*Elemente de dinamica sateliţilor GPS*", Editura Academiei Navale „Mircea cel Bătrân", Constanţa, 1999
25. Cojocaru, S., „*Tratat de navigaţie maritimă – Metodele moderne ale navigaţie maritime*", Editura Ars Academica, Bucureşti, 2008

26. Cojocaru S., Dragușan A., Lupu S., "*Upon a possible common geostationary and GPS constellation: a dynamical investigation*", Recent Insights into our Universe Workshop, 28-29 Oct 2009, Bucuresti,
27. Dinescu, A., "*Introducere în geodezia geometricã spaţială*", Ed.Tehnică, Bucureşti 1980
28. Drăgușan A., Contribuții la teoria mișcării sateliților ecuatoriali, Teză de doctorat, Institutul Astronomic, Bucureşti 2008
29. Drăguşan, A., Lupu, S., „*Methods for representing the gravitational potential*", Romanian Astronomical Journal, vol.16 Supplement, p.127, 2005
30. Drăguşan, A., Lupu, S., „*EPIRB Distress Signal Via Satellite*", Romanian Astronomical Journal, 2006
31. Drăguşan, A., Lupu, S., Cojocaru S., „*Astronomical Principles of Satellite Positioning*", Exploring the solar system and the Universe, American Institute of Physics, 2008
32. Escobal, P. R., „*Methods of orbit determination*", New York, 1965
33. Eriksson, P., „*Orbital and attitude perturbation on a small satellite*", 2002
34. Expertier, P., "*Geopotential from space techniques*", Celestial Mechanics and Dynamical Astronomy, 1994
35. Farinella, P. Et al., „*Dynamics of an artificial satellite in an Earth-fixed reference frame: efect of polar motions in Reference Coordinate Systems for Earth Dynamics*", ed. E M Gasposchkin and B Kolaczek (Dordrecht: Reidel) 1981
36. Garfinkel, B., "*The Orbit of a Satellite of an Oblate Planet*", The Astronomical Journal, vol.64, 1959
37. Geyling F., Wersterman R., "*Introduction to orbital mechanics*", Canada, 1971
38. Gube, M., „*Planetary albedo estimates from Meteosat data*", ESA Journal 1982
39. Heiskanen and Moritz, "*Physical Geodesy*", Technical University of Graz, 1967
40. Hofmann-Wellenhof, B. et al, „*GPS - Theory and Practice*", New York 1993.
41. Huang, S.S., "*Some Dynamical properties of natural and artificial satellites*", The Astronomical Journal,1961
42. Iacob, C., "*Mecanica teoretică*", Ed. Didactică şi Pedagogică, Bucureşti 1980
43. Jamet O., Thomas E., „*A linear algorithm for computing the spherical harmonic coefficients of the gravitational potential from a constant density polyhedron*", Institut Geographique National, Laboratoire de Recherche en Geodesie, 2004
44. Kaula, W.M., "*Development of the lunar and solar disturbing functions for a close satellite*", The Astronomical Journal, 1962
45. Kaula, W.M., "*Theory of satellite geodesy*", Blaisdell Publ.Co., Waltham 1966
46. Kovalevsky, J., "*Introduction to the celestial mechanics*", Olanda, 1967
47. Kovalevsky, J., Mueller, Kolaczek, „*Reference Frames in Astronomy and Astrophysics*", Kluwer Academics, 1989.
48. Kozai, Y., "*Numerical Results from Orbits*", Smithsonian Astrophysical Observatory, Special Report 101, 1962
49. Kozai, Y., "*Revised zonal harmonics in the geopotential*", SAO Special Report, 1969
50. Lala, P., Sechnal, L., "*The Earth Shadowing Effects in the Short - Periodic Perturbations of the Satellite Orbits*", BAC, 1969
51. Levallois, J.J., Kovalevsky, J., "*Geodesie Generale*", Tome IV, Paris 1971
52. Lupu S., Zaharescu E., *Effects of direct and indirect solar radiation pressure in orbital parameters of GPS satelittes*, Analele Univ. Ovidius Constanţa, Seria Matematică, ISSN 1224-1784, Vol. 22(2), 2014, 141-150, DOI: 10.2478/auom-2014-0039
53. Lupu E.C., Lupu S., Adina Petcu, *EB lifetime distributions as alternative to the EP lifetime distributions*, Analele Univ. Ovidius Constanţa, Seria Matematică, ISSN 1224-1784, Vol. 22(3), 2014, 115-125, DOI: 10.2478/auom-2014-0053

54. Lupu S. „*Elemente de dinamica sistemului global de poziționare NAVSTAR - GPS*”, Ed. Academiei Navale “Mircea cel Bătrân”, Constanța 2011
55. Lupu S. - *The evaluation of gravitational perturbation acceleration actions on GPS satellites*, Constanta Maritime University’s Annals, Volume 18 - 2012, Ed. Nautica, ISSN 1582 – 3601
56. Lupu S. - *The effects caused by non-gravitational perturbations: the anisotropic thermal emission and antennas emission on GPS satellites*, Constanta Maritime University’s Annals, Volume 18 - 2012, Ed. Nautica, ISSN 1582 – 3601
57. Lupu S., Pocora A., Lupu E.C. – *Modelling the eclipse region for GPS satellites*, “Mircea cel Batran” Naval Academy Scientific Bulletin, Volume XV – 2012 – Issue 1 Published by “Mircea cel Batran” Naval Academy Press, Constanta, ISSN 1454-864X
58. Lupu S., Lupu E.C., Crețu G. – *Some remarks on GPS satellites orbites*, “Mircea cel Batran” Naval Academy Scientific Bulletin, Volume XIV – 2011 – Issue 2 Published by “Mircea cel Batran” Naval Academy Press, Constanta, ISSN 1454-864X
59. Manakov, Yu. M., „*Perturbing effect of terrestrial thermal radiation pressure on an artificial Earth satellite Geodesy*”, Mapping and Photogrammetry 1977
60. Mathuna D., „*Integrable systems in celestial mechanics*”, Springer, SUA, 2008
61. McFadden L.A., Weissman P.R., Johnson T.V., „*Encyclopedia of the Solar System*”, Academic Press, 2007
62. Milani, A., and all, „*Non-gravitational perturbations and satelitte geodesy*”, Dipartamento di Matematica, Universita di Pisa, Adam Hilger, Bristol, 1987
63. Milone E., Wilson W., “*Solar system astrophysics*”, Springer, New York, 2008
64. Mioc, V., Radu, E., “*Aerodynamic Drag Perturbations in Artificial Satellite Nodal Period*”, Astron.Nachr., **5**, p.327-334, 1991
65. Mioc, V., Radu, E., “*A complete first-order approximation for the motion in a noncentral attraction field*”, Rev. d′Analyse Num.et de Theorie de l′Approx., 1993
66. Mioc, V., Stoica, C., “*The Schwarzschild problem in astrophysics*”, 1997
67. Mioc, V., “*Teza de doctorat*”, Universitatea Babeş Boliay, Cluj-Napoca 1980
68. Moore P., “*The data book of astronomy*”, Institute of Physics, SUA, 2000
69. Mueller, I., “*Spherical and Practical Astronomy*”, Frederick Ungar Publ. Co., New York 1969
70. Munyamba, N. “*Derivation of a Solar Radiation Pressure Model of the latest GLONASS Spacecraft*”, 2010
71. Murray C., *Solar system dynamics*, 1999
72. Nakiboglu, S.M., Krakiwski, E.J., Schwary. K.P., Buffet, B., Wanless, B., „*a multi-station, multi-pass approach to Global Positioning System improvement and precise positioning*”, Geodesy Survey of Canada, Rep. 85-003, Ottawa 1985
73. Pal, A., Ureche, V., “*Astronomie*”, Ed.Didacticã şi Pedagogicã, Bucureşti 1983
74. Rodrigues-Solano, C. Master Thesis: „*Impact of albedo modelling on GPS orbits*”, 2009
75. Rodrigues-Solano, C. Et al. „*Estimating on-orbit optical properties for GNSS satellites*”, Bremen 2010
76. Seeber, G., „*Satellite Geodesy - Foundations, Methods and Applications*”, Berlin, 1993
77. Sehnal, L., „*Effects of the terrestrial infrared radiation pressure on the motion of an artificial satellite*”, Celestial Mech. 1981
78. Sehnal, L., “*The Theory of Orbits in the Solar System and in Stellar Systems*”, IAU Symposium, Thessaloniki, Academic Press 1964
79. Syma A., Thesis: “*Thermal Re-Radiation Modelling for the Precise Prediction and Determination of Spacecraft Orbits*”, 2005
80. Smith, D. E., „*Earth-reflected radiation pressure in Dynamics of Satellites*”, ed. B Morando (Berlin: Springer) 1970

81. Su, H., “*Precise orbit determination of global navigation satellite system of second generation*”, Germania, 2000
82. Tataru N., Lupu S. „*The optimization of the calculus of the distances on the electronic charts*”, Buletinul Institutului Politehnic Iaşi, Tomul LII (LVI), Fasc. 5, 2006
83. Tscherning, C.C., Sanso, M., „*Prediction of spherical harmonic coefficients using Least-Squares Collocation*”, Copenhagen, Danemarca, 2000
84. Vascoviak, S.N., ′Funcția Teni b Zadace o Vlianii Svetogo Davlenia na Dviscenie′, *V.M.U., Ser. fiz.-astr.*, **5**, p.584, 1974.
85. Zierbart M., Thesis: “*Hight Precision Analitical Solar Radiation Pressure Modelling for GNSS Spacecraft*”, 2001
86. Xu G., „*GPS Theory, Algorithms and applications*”, Springer, Germania, 2007
87. Xu G., „*Orbits*”, Springer, Germania, 2008
88. Wolf, R., “*Satellite orbit and ephemeris determination using inter satellite link*”, Germania, 2000
89. ftp://tycho.usno.navy.mil/pub/gps/
90. http://www.bsu.edu
91. http://ceres-tool.larc.nasa.gov/org_tool/srbavg
92. http://www.esa.int
93. http://www.hyperphysics.phy-astr.gsu.edu
94. http://www.icgem.gfz-postdam.de
95. http://www.iers.org
96. http://igs.org/igscb/product/1780/
97. http:// www.imcce.fr/en/ephemerides/formulaire
98. http://www.nasa.gov
99. http://www.scienceworld.wolfram.com
100. http://www.spaceandtech.com
101. *** *IERS Annual Report 2001*”, International Earth Rotation Service, Verlag des Bundesamts für Kartographie und Geodäsie, Frankfurt am Main 2002
102. GRANT - *„Studiul erorilor orbitale ale sateliţilor de poziţionare GPS”* poz. 80 din Planul Sectorial de Cercetare Dezvoltare al Ministerului Apărării Naționale pe anul 2009